HYDRAULICS AND STABILITY OF MULITPLE INLET-BAY SYSTEMS: ST. ANDREW BAY, FLORIDA

By

MAMTA JAIN

A THESIS PRESENTED TO THE GRADUATE SCHOOL
OF THE UNIVERSITY OF FLORIDA IN PARTIAL FULFILLMENT
OF THE REQUIREMENTS FOR THE DEGREE OF
MASTER OF SCIENCE

UNIVERSITY OF FLORIDA

2002

ACKNOWLEDGMENTS

The author would like to express her deepest and heartiest thanks to her advisor and chairman of the supervisory committee, Dr. Ashish Mehta, for his assistance, encouragement, moral support, guidance and patience throughout this study. Special thanks go to committee member Dr. Robert Dean for his help and advice in solving the hydraulic model equations. Gratitude and thanks are also extended to the other members of the committee, Dr. Robert Thieke and Dr. Andrew Kennedy, for their guidance and assistance. Thanks go to Dr. J. van de Kreeke for his help in solving the linearized lumped parameter model for the stability of inlets.

Assistance provided by Michael Dombrowski of Coastal Tech, for whom the hydrographic surveys were carried out, is sincerely acknowledged. Thanks go to Sidney Schofield and Vic Adams, for carrying out the fieldwork.

The author wishes to acknowledge the assistance of Kim Hunt, Becky Hudson, and the entire Coastal and Oceanographic Engineering Program faculty and staff for their encouragement and emotional support.

The author would like to thank her husband, Parag Singal, for his love, encouragement and support, and her parents and family for providing her with mind, body and soul.

Last, but not least, the author would like to thank the eternal and undying Almighty who provides the basis for everything and makes everything possible.

TABLE OF CONTENTS

LIST OF TABLES

LIST OF FIGURES

LIST OF SYMBOLS

Symbols

A_B, A_{B1}, A_{B2}, A_{B3}	bay water surface areas at MSL
A_c A_{c1}, A_{c2}, A_{c3}, A_{c4}	flow cross-sectional areas of inlets
a_o	ocean (Gulf) tide amplitude
a_B, a_{B1}, a_{B2}, a_{B3}	bay tide amplitudes
$\hat{a}_B$, $\hat{a}_{B1}$, $\hat{a}_{B2}$ $\hat{a}_{B3}$	dimensionless bay tide amplitudes
a_i	constant that relates hydraulic radius with area of triangular cross-section
a, b, c, A, B	constants defined to solve system of equations
B_i	dimensionless resistance factor
C, C_1, C_2, C_3, C_4	coefficients in linear relations of inlet hydraulics
C_D, C_{DL1}, C_{DL2}, C_{DL3}, C_{DL4}	linear discharge coefficients
C_K	prism correction coefficient of Keulegan
f	Darcy-Weisbach friction factor
F	friction coefficient
g	acceleration due to gravity
h_k	kinetic head
i	subscript specifying the inlet under consideration
K	Keulegan coefficient of filling or repletion
k	bottom roughness

k_{en}	entrance loss coefficient
k_{ex}	exit loss coefficient
L_c, L_1, L_2, L_3, L_4	channel lengths
m	sum of entrance and exit losses.
P	tidal prism
Q, Q_1, Q_2, Q_3, Q_4	discharges through inlets
Q_m	peak discharge
R, R_1, R_2, R_3, R_4	hydraulic radii
R_t	bay tide range
R_o	ocean (Gulf) tide range
r_1, r_2, r_3	polar representation of the bay tides
T	tidal period
t	time
u	velocity
u_B	bay current velocity
u_c, u_{c1}, u_{c2}, u_{c3}, u_{c4}	velocities through inlets
u_{eqi}	equilibrium velocity of inlet
u_{max1}, u_{max2}, u_{max3}, u_{max4}	maximum velocities through inlets
u_o	ocean (Gulf) current velocity
X	distance between UF and NOS tide stations
α_o, α_B	velocity coefficients
ε_{B1}, ε_{B2}, ε_{B3}	high water (HW) or low water (LW) lags
ε_{v1}, ε_{v2}, ε_{v3}, ε_{v4}	inlet velocity lags

γ	specific time when sea is at MSL
θ	dimensionless time
η	water elevation
η_o	ocean (Gulf) tide elevation with respect to MSL
η_B, η_{B1}, η_{B2}, η_{B3}	bay tide elevations with respect to MSL
$\hat{\eta}_B$, $\hat{\eta}_{B1}$, $\hat{\eta}_{B2}$, $\hat{\eta}_{B3}$	dimensionless bay tide elevations
$\hat{\tau}$	maximum bottom shear stress
$\hat{\tau}_{eq}$	equilibrium shear stress

Abstract of Thesis Presented to the Graduate School
of the University of Florida in Partial Fulfillment of the
Requirements for the Degree of Master of Science

HYDRAULICS AND STABILITY OF MULTIPLE-INLET BAY SYSTEMS:
ST. ANDREW BAY, FLORIDA

By

Mamta Jain

December 2002

Chairman: Ashish J. Mehta
Major Department: Civil and Coastal Engineering

Tidal inlets on sandy coasts are subject to the continuous changes in their geometry and as a result influence shorelines in the vicinity. Since engineering modifications carried out at one inlet can affect the long-term stability of others in the vicinity of the modified inlet, it is important to understand the stability of all inlets connecting a bay to the ocean. Inlet stability is related to the equilibrium between the inlet cross-sectional area and the hydraulic environment.

St. Andrew Bay on the Gulf of Mexico coast of Florida's panhandle is part of a three-bay and two- ("ocean") inlet complex. One of these inlets is St. Andrew Bay Entrance and the other is East Pass, both of which are connected to St. Andrew Bay on one side and the Gulf on the other. Historically, East Pass was the natural connection between the bay and the Gulf. In 1934, St. Andrew Bay Entrance was constructed 11 km west of East Pass to provide a direct access between the Gulf and Panama City. Due to the long-term effect of this opening of St. Andrew Bay Entrance, East Pass closed

naturally in 1998. A new East Pass was dredged open in December 2001, and the objective of the present study was to examine the hydraulics and stability of this system of two sandy ocean inlets connected to interconnected bays.

To study the system as a whole, a linearized hydraulic model was developed for a three-bay and four-inlet (two ocean and the other two connecting the bays) system and applied to the St. Andrew Bay system. To investigate the stability of the ocean inlets, the hydraulic stability criterion was extended to the two-ocean inlets and one (composite) bay system using the linearized lumped parameter model. The following conclusions are drawn from this analysis.

The linearized hydraulics model is shown to give good results--the amplitudes of velocities and bay tides are within ±5%. The percent error for St. Andrew Bay is almost zero, and for the other bays it is within ±20%.

The stability model gives the qualitative results. The bay area has a significant effect on the stability of the two inlets. At a bay area of 74 km^2 (the actual area of the composite bay), both inlets are shown to be unstable. Increasing the area by 22% to 90 km^2 stabilizes St. Andrew Bay Entrance, and by 42% to 105 km^2 stabilizes East Pass as well. Keeping the bay area at 105 km^2 and increasing the length of East Pass from 500 m to 2000 m destabilizes this inlet because as the length increases the dissipation in the channel increases as well.

CHAPTER 1
INTRODUCTION

1.1 Problem Definition

Tidal inlets are the relative short and narrow connections between bays or lagoons and the ocean or sea. Inlets on sandy coasts are subject to the continuous changes in their geometry. Predicting the adjustment of the inlet morphology after a storm event in particular, i.e., whether the inlet will close or will remain open, requires knowledge of the hydraulic and sedimentary processes in the vicinity of the inlet. These processes are governed by complex interactions of the tidal currents, waves, and sediment. In spite of recent advances in the description of flow field near the inlet and our understanding of sediment transport by waves and currents (Aubrey and Weishar 1988), it is still not possible to accurately predict the morphologic adjustment of the inlet to hydrodynamic forcing.

Inlet stability is dependent upon the cumulative result of the actions of two opposing factors, namely, a) the near-shore wave climate and associated littoral drift, and b) the flow regime through the inlet. Depending on the wave climate and the range of the tide, one of these two factors may dominate and cause either erosion or accumulation of the sand in the inlet. However, on a long-term basis, a stable inlet can be maintained only if the flow through the inlet has enough scouring capacity to encounter the obstruction against the flow due to sand accumulation, and to maintain the channel in the state of non-silting, non-scouring equilibrium. If such is not the case and waves dominate, then the accumulated sand will begin to constrict the inlet throat, thereby reducing the tidal

prism. The resulting unstable inlet may migrate or orient itself at an angle with the shoreline depending on the predominant direction of the littoral drift; the channel may elongate, thereby increasing the frictional resistance to the flow, and finally, a stage may be reached when perhaps a single storm could close the inlet in a matter of hours.

Stability criteria based on inlet hydraulics and sediment transport for single inlets have been proposed by, among others, O'Brien (1931), Escoffier (1940), O'Brien and Dean (1972), Bruun (1978) and Escoffier and Walton (1979). All criteria assume that sufficient sand is available to change the inlet channel geometry in response to the prevailing hydrodynamic conditions. These investigators found various stability parameters to describe the stability of the inlet. It should be noted, however, that while it is relatively easy to deal with the stability of single inlets, the problem becomes complex when, as is commonly the case, more than one inlet connect the ocean to a single bay or more than one interconnected bays. Some examples of such systems are as follows.

Three cases of the history of two inlets in a bay are worthy of citation. One case is that of Boca Ciega Bay on the Gulf coast of Florida, where the co-dependency of two inlets, Blind Pass and Johns Pass, appears to be reflected in the history of their cross-sectional areas. While Blind Pass has historically been narrowing due to shoaling, John's Pass has been increasing in size, as shown in Table 1.1. As a result, Blind Pass now requires regular dredging for its maintenance while severe bed erosion has occurred at John's Pass (Mehta, 1975; Becker and Ross, 2001).

Another example is that of St. Andrew Bay Entrance and the East Pass. As mentioned previously, East Pass used to be a large inlet and was the only natural connection between the Gulf of Mexico and the St. Andrew Bay. In 1934, St. Andrew

Bay entrance was constructed 11 km west of East Pass through the barrier island by the federal government to provide a direct access between the Gulf and Panama City. Table 1.2 gives the cross-sectional area of each inlet over time.

Table 1.1 Cross-sectional areas of Johns Pass and Blind Pass in Boca Ciega Bay

Year	Area (m^2)		Hydraulic Radius (m)	
	John's Pass	Blind Pass	John's Pass	Blind Pass
1873	474	538	3.7	3.5
1883	432	496	3.8	3.0
1926	531	209	3.9	1.9
1941	636	225	4.1	1.4
1952	849	157	4.6	2.7
1974	883	411	4.9	1.6
1998	950	230	5.3[d]	0.9[d]

[d] Estimated by assuming no change in channel width since 1974.

Table 1.2 Cross-sectional areas of St. Andrew Bay Entrance and East Pass

Year	Area (m^2)	
	St. Andrew Bay Entrance	East Pass
1934	1,835	3,400
1946	3,530	2,146
1983	3,943	1,392
1988	-	Closed
2001	5,210	Reopened

The third example is that of Pass Cavallo and Matagorda Inlet connecting Matagorda Bay, Texas, to the Gulf. Stability analysis carried out by van de Kreeke (1985) on this system showed that Pass Cavallo is an unstable inlet, which is decreasing in cross-section, whereas Matagorda Inlet is increasing in size. The areas of cross-sections of the two inlets are listed in Table 1.3.

Table 1.3 Cross-sectional areas of Pass Cavallo and Matagorda Inlet

Year	Area (m^2)	
	Pass Cavallo	Matagorda Inlet
1959	8,000	Closed
1970	7,500	3,600

The above sets of complex problems are dealt with in this study in a simplified manner, with the following objective and associated tasks.

1.2 Objective and Tasks

The main objective of this study is to examine the hydraulics and thence the stability of a system of two sandy ocean inlets connected to interconnected bays. The sequence of tasks carried out to achieve this goal is as follows:

1. Deriving the basic hydraulic equations using the linearized approach for a complex four inlets and three bays system.
2. Solving these equations, applying them to the St. Andrew Bay system, and comparing the results with those obtained from the hydrographic surveys.
3. Developing stability criteria using the basic Escoffier (1940) model for one inlet and one bay and then extending this model to the two inlets and a bay.
4. Carrying out stability analysis for *N* inlets and a bay using the linearized lumped parameter model of van de Kreeke (1990), and then applying it to the St. Andrew Bay system.

1.3 Thesis Outline

Chapter 2 describes the hydraulics of the multiple inlet-bay system. It progresses from the basic theory to the development of linearized models for simple and complex systems. Chapter 3 describes the stability of the system, including an approximate method to examine multiple inlets in a bay. Chapter 4 includes details of hydrographic surveys and summarizes the data. Chapter 5 discusses the input and output parameters required for the calculation. It also presents the results. All calculations are given in the appendices. Conclusions are made in Chapter 6, followed by a bibliography and a biographical sketch of the author.

CHAPTER 2
HYDRAULICS OF A MULTIPLE INLET BAY SYSTEM

2.1 Governing Equations of an Inlet-Bay System

2.1.1 System Definition

The governing equations for a simple inlet-bay system may be derived by considering the inlet connecting the ocean and the bay as shown in Figure 2.1.

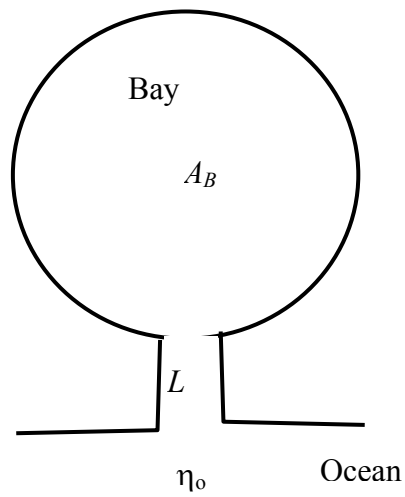

Figure 2.1 One bay and one inlet system

These equations are derived subjected to the following assumptions.

1 The inlet and bay banks are vertical.

2 The range of tide is small as compare to the depth of water everywhere.

3 The bay surface remains horizontal at all times, i.e., the tide is "in phase" across the bay. That means the longest dimension of the bay be small compared to the travel time of tide through the bay.

4 The mean water level in the bay equals that in the ocean.

5 The acceleration of mass of water in the channel is negligible.

6 There is no fresh water inflow into the bay.

7 There is no flow stratification due to salinity.

8 Ocean tides are represented by a periodical function.

2.1.2 Energy Balance

Applying the energy balance between ocean and bay one gets

$$\eta_o + \alpha_o \frac{u_o^2}{2g} = \eta_B + \alpha_B \frac{u_B^2}{2g} + \sum \Delta h \tag{2.1}$$

where

η_o = Ocean tide elevation with respect to mean sea level,

η_B = Bay tide elevation with respect to mean sea level,

u_o = Ocean current velocity,

u_B = Bay current velocity,

α_o and α_B = Coefficients greater than one which depend on the spatial distribution of u_o and u_B, respectively,

$\Sigma\Delta h$ = Total head loss between the ocean and the bay, and

g = acceleration due to gravity.

It is also assumed that ocean and bay are relatively deep; thus u_o and u_B are small enough to be neglected. Then Eq. (2.1) becomes

$$\sum \Delta h = \eta_o - \eta_B \tag{2.2}$$

There are generally two types of head losses. One includes concentrated or "minor losses" due to convergence and divergence of streamlines in the channel. The second type is gradual loss due to bottom friction in the channel. The entrance and exit losses may be written in terms of the velocity head $\frac{u_c^2}{2g}$ in the channel, with the entrance loss coefficient k_{en} and the exit loss coefficient k_{ex}, i.e.,

$$\text{Entrance loss} = k_{en}\frac{u_c^2}{2g} \tag{2.3}$$

$$\text{Exit loss} = k_{ex}\frac{u_c^2}{2g} \tag{2.4}$$

where u_c is the velocity through the inlet. Gradual energy losses per unit length depend on the channel roughness and are given in form of Darcy-Weisbach friction factor

$$\text{Gradual loss} = \frac{fL}{4R}\frac{u_c^2}{2g} \tag{2.5}$$

where

f = Darcy-Weisbach friction coefficient,

R = hydraulic radius of channel, and

L = Length of channel.

Substitution of Eqs. (2.3), (2.4) and (2.5) into (2.2) gives

$$\eta_o - \eta_B = \frac{u_c^2}{2g}\left(k_{en} + k_{ex} + \frac{fL}{4R}\right) \tag{2.6}$$

or

$$u_c = \sqrt{\frac{2g}{k_{en} + k_{ex} + \frac{fL}{4R}}}\sqrt{|\eta_o - \eta_B|}.sign\left(\eta_o - \eta_B\right) \tag{2.7}$$

The $sign(\eta_0 - \eta_B)$ term must be included since the current reverses in direction every half tidal cycle.

2.1.3 Continuity Equation

The equation of continuity, which relates the inlet flow discharge to the rate of rise and fall of bay water level, is given as

$$Q = u_c A_c = \frac{d}{dt}\left(A_B \eta_B\right) \tag{2.8}$$

where

Q = flow rate through the inlet,

A_c = Inlet flow cross-sectional area, and

A_B = bay surface area.

Therefore Eq. (2.8) becomes

$$u_c = \frac{A_B}{A_c}\frac{d\eta_B}{dt} \tag{2.9}$$

Eliminating u_c between Eq. (2.7) and (2.9) leads to

$$\frac{d\eta_B}{dt} = \frac{A_c}{A_B}\sqrt{\frac{2g}{k_{en} + k_{ex} + \frac{fL}{4R}}}\sqrt{|\eta_o - \eta_B|}.sign\left(\eta_o - \eta_B\right) \tag{2.10}$$

Next, we introduce the dimensionless quantities

$$\hat{\eta}_o = \frac{\eta_o}{a_o};\ \hat{\eta}_B = \frac{\eta_B}{a_o};\ \theta = \frac{2\pi t}{T} = \sigma t \tag{2.11}$$

where a_o = ocean tide amplitude (one-half the ocean tidal range), T = tidal period and σ = tidal (angular) frequency. Substitution into Eq. (2.10) gives

$$\frac{d\hat{\eta}_B}{d\theta} = K\sqrt{|\hat{\eta}_o - \hat{\eta}_B|}.sign\left(\hat{\eta}_o - \hat{\eta}_B\right) \tag{2.12}$$

where

$$K = \frac{T}{2\pi a_o}\frac{A_c}{A_B}\sqrt{\frac{2ga_o}{k_{en} + k_{ex} + \frac{fL}{4R}}} \tag{2.13}$$

in which K is referred to as the "coefficient of filling or repletion" (Keulegan, 1967). Keulegan solved the first order differential equation, Eq. (2.12), for $\hat{\eta}_B$ in terms of the repletion coefficient K and dimensionless time θ using numerical integration.

2.2 The Linearized Method

A linear method was suggested by Dean (1983) for solving Eq. (2.12). For this approach it was assumed that the velocity u_c in Eq. (2.7), is proportional to the head difference (η_o - η_B) rather than the square root of the head difference, according to

$$u_c = \sqrt{\frac{2g}{a_o}} C_{DL} \left(\eta_o - \eta_B \right) \tag{2.14}$$

where C_{DL} = "linear discharge coefficient." This coefficient is defined as

$$C_{DL} = \frac{1}{\sqrt{k_{en} + k_{ex} + \frac{fL}{4R}}} \sqrt{\frac{a_o}{\left(\eta_o - \eta_B \right)_{\max}}} \tag{2.15}$$

where $(\eta_o - \eta_B)_{max}$ is the maximum head difference across the inlet. Now, combining Eqs. (2.14), (2.9) and (2.11), Eq. (2.12) can be written in terms of the linear relationship as

$$\hat{\eta}_o - \hat{\eta}_B = \frac{\sigma}{C} \left[\frac{d\hat{\eta}_B}{d\theta} \right] \tag{2.16}$$

where

$$C = C_{DL} \frac{A_c}{A_B} \sqrt{\frac{2g}{a_o}} \tag{2.17}$$

Under assumption (8) the ocean tide is assumed to be periodic. Because of the linear assumption the bay tide is also periodic, it can be written as

$$\hat{\eta}_o = \cos\theta \tag{2.18}$$

$$\hat{\eta}_{B1} = \hat{a}_{B1} \cos(\theta - \varepsilon_{B1}) \tag{2.19}$$

where $\hat{a}_B = \dfrac{a_B}{a_o}$, a_B = one-half the bay tide range (i.e., bay tide amplitude) and ε_B = lag between high water (HW) or low water (LW) in the ocean and the corresponding HW or LW in the bay.

Eq. (2.18) and Eq. (2.19) are next substituted into Eq. (2.16) and the following complex number technique is used to solve for a_B and ε_B:

1 Define the following constants:

$$\frac{\sigma}{C} = a\,,\ \hat{\eta}_o = \mathrm{Re}\left(e^{i\theta}\right)$$

2 Let the following variables be represented in the polar form:

$$\hat{\eta}_{B1} = \mathrm{Re}\left(\hat{a}_{B1} e^{i(\theta - \varepsilon_{B1})}\right) = r_1$$

3 Therefore

$$\frac{d\hat{\eta}_B}{d\theta} = ir_1$$

4 So the equations are reduced to

$$1 = (1 + ai)r_1 \tag{2.20}$$

$$r_1 = \frac{1}{1+ai}\,;\ \mathrm{Re}(r_1) = \frac{1}{1+a^2}\,;\ \mathrm{Im}(r_1) = \frac{-a}{1+a^2}$$

where

Re(r_1) = is the real part of the solution, and

Im(r_1) = is the imaginary part of the solution.

The magnitude of r_1 represents $\hat{a}_{B1}$ and the phase lag ε_{B1} is represented by the angle of r_1:

$$\hat{a}_{B1} = \frac{1}{\sqrt{1+a^2}} \tag{2.21}$$

$$\varepsilon_{B1} = \tan^{-1} a \tag{2.22}$$

The velocity u_{c1} through inlet 1 is therefore given by

$$u_{c1} = u_{\max 1} \cos\left(\theta - \varepsilon_{v1}\right) \tag{2.23}$$

where u_{max1} is the maximum velocity through inlet 1, ε_{v1} is the phase lag between the velocity in inlet 1 and HW or LW in the ocean.

Substituting for η_o and η_{B1} from Eq. (2.18) and Eq. (2.19) in Eq. (2.14) and combining Eqs. (2.23) and (2.14) we get the required expression for u_{max1}. It should be noted that velocity is out of phase with respect to displacement by $\pi/2$. Therefore, $\varepsilon_{v1} = \varepsilon_{B1} - \pi/2$.

2.3 Multiple Inlet-Bay System.

2.3.1 Two Inlets and Two Bays with One Inlet Connected to Ocean

In the case of two bays with one inlet connecting to the ocean and the second connecting the bays as shown in Figure 2.2, the eight assumptions mentioned in section 2.1.1 and the linear relationship both hold. In a manner similar to that employed for a single inlet-bay case, the velocity relationship and the equation of continuity for two-bay system may be written with reference to the notation of Figure 2.2.

Thus the following relationships are obtained:

$$u_{c1} = \sqrt{\frac{2g}{a_o}} C_{DL1}\left(\eta_o - \eta_{B1}\right) \tag{2.24}$$

$$Q_1 = u_{c1} A_{c1} = A_{B1} \frac{d\eta_{B1}}{dt} + A_{B2} \frac{d\eta_{B2}}{dt} \tag{2.25}$$

$$u_{c2} = \sqrt{\frac{2g}{a_{B1}}} C_{DL2}\left(\eta_{B1} - \eta_{B2}\right) \tag{2.26}$$

$$Q_2 = u_{c2} A_{c2} = A_{B2} \frac{d\eta_{B2}}{dt} \tag{2.27}$$

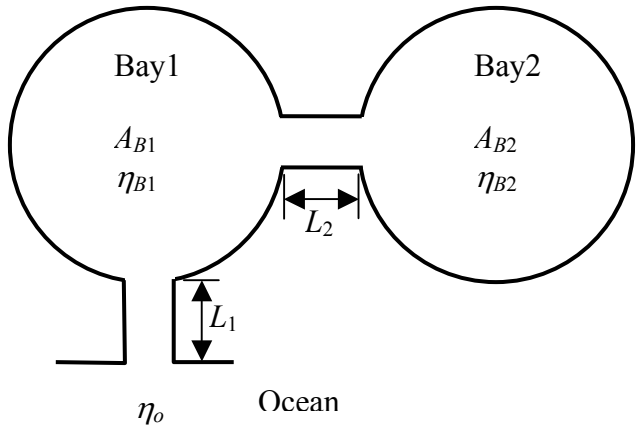

Figure 2.2 Two bays and two inlets with one inlet connected to ocean.

where

u_{c1}, u_{c2} = velocities through the inlets 1 and 2,

Q_1, Q_2 = discharges through inlets 1 and 2,

A_{c1}, A_{c2} = inlet flow cross-sectional areas, and

A_{B1}, A_{B2} = bay water surface areas.

$$C_{DL1} = \frac{1}{\sqrt{k_{en} + k_{ex} + \frac{fL_1}{4R_1}}} \sqrt{\frac{a_o}{(\eta_o - \eta_{B1})_{\max}}} \tag{2.28}$$

$$C_{DL2} = \frac{1}{\sqrt{k_{en} + k_{ex} + \frac{fL_2}{4R_2}}} \sqrt{\frac{a_{B1}}{(\eta_{B1} - \eta_{B2})_{\max}}} \tag{2.29}$$

where

L_1, L_2 = inlet lengths, and

R_1, R_2 = hydraulic radii of the channels.

Eliminating u_{c1} between Eq. (2.24) and Eq. (2.25) gives

$$\eta_o - \eta_{B1} = \frac{1}{C_1}\left[\frac{d\eta_{B1}}{dt} + \frac{A_{B2}}{A_{B1}}\frac{d\eta_{B2}}{dt}\right] \tag{2.30}$$

where

$$C_1 = C_{DL1} \frac{A_{c1}}{A_{B1}} \sqrt{\frac{2g}{a_o}} \tag{2.31}$$

Combining Eq. (2.26) and Eq. (2.27) yields

$$\eta_{B1} - \eta_{B2} = \frac{1}{C_2} \left[\frac{d\eta_{B2}}{dt} \right] \tag{2.32}$$

where

$$C_2 = C_{DL2} \frac{A_{c2}}{A_{B2}} \sqrt{\frac{2g}{a_{B1}}} \tag{2.33}$$

The dimensionless ocean tide is given by Eq. (2.18), and the dimensionless tides in bays 1 and 2 now become

$$\hat{\eta}_{B1} = \hat{a}_{B1} \cos(\theta - \varepsilon_{B1}) \tag{2.34}$$

$$\hat{\eta}_{B2} = \hat{a}_{B2} \cos(\theta - \varepsilon_{B2}) \tag{2.35}$$

where

$$\hat{a}_{B1} = \frac{a_{B1}}{a_o}$$

a_{B1} = one-half the tide range (i.e., amplitude) in bay 1.

$$\hat{a}_{B2} = \frac{a_{B2}}{a_o}$$

a_{B2} = one-half the tide range (i.e., amplitude) in bay 2.

ε_{B1} = lag between high water (HW) or low water (LW) in the ocean and corresponding HW or LW in the bay 1.

ε_{B2} = lag between high water (HW) or low water (LW) in the ocean and corresponding HW or LW in the bay 2.

Eq. (2.30) and Eq. (2.32) can be expressed in the dimensionless form as

$$\hat{\eta}_o - \hat{\eta}_{B1} = \frac{\sigma}{C_1}\left[\frac{d\hat{\eta}_{B1}}{d\theta} + \frac{A_{B2}}{A_{B1}}\frac{d\hat{\eta}_{B2}}{d\theta}\right] \tag{2.36}$$

$$\hat{\eta}_{B1} - \hat{\eta}_{B2} = \frac{\sigma}{C_2}\left[\frac{d\hat{\eta}_{B2}}{d\theta}\right] \tag{2.37}$$

The above equations are solved by the matrix method assuming the variables to be complex numbers. The solution is obtained as follows:

1 Define the following constants

$$\frac{\sigma}{C_1} = a\,,\ \frac{\sigma}{C_2} = b\,,\ \frac{A_{B2}}{A_{B1}} = A\,,\ \hat{\eta}_o = \mathrm{Re}\left(e^{i\theta}\right)$$

2 Let

$$\hat{\eta}_{B1} = \mathrm{Re}\left(\hat{a}_{B1}e^{i(\theta-\varepsilon_{B1})}\right) = r_1,\ \hat{\eta}_{B2} = \mathrm{Re}\left(\hat{a}_{B2}e^{i(\theta-\varepsilon_{B2})}\right) = r_2\,, \frac{d\hat{\eta}_{B1}}{d\theta} = ir_1,\ \frac{d\hat{\eta}_{B2}}{d\theta} = ir_2$$

3 So the equations are reduced to

$$1 = (ai+1)r_1 + aAir_2 \tag{2.38}$$

$$0 = -r_1 + (bi+1)r_2 \tag{2.39}$$

4 In the matrix form they become

$$\begin{pmatrix} 1 \\ 0 \end{pmatrix} = \begin{pmatrix} r_1 \\ r_2 \end{pmatrix}\begin{pmatrix} ai+1 & aAi \\ -1 & bi+1 \end{pmatrix} \tag{2.40}$$

5 The solution is

$$r_1 = \frac{-i\left(b-i\right)}{X} \tag{2.41}$$

$$r_2 = \frac{-1}{X} \tag{2.42}$$

where

$$X = (ab-1) - i(aA+a+b)\,;\ \overline{X} = (ab-1) + i(aA+a+b)$$

$$X\overline{X} = (ab-1)^2 + (aA+a+b)^2$$

$$\mathrm{Re}(r_1) = \frac{b\left(b+a+aA\right)-(ab-1)}{X\overline{X}}\,;\ \mathrm{Im}(r_1) = \frac{-b\left(ab-1\right)-\left(a+b+aA\right)}{X\overline{X}}$$

$$\mathrm{Re}(r_2) = \frac{-(ab-1)}{X\overline{X}}\,;\ \mathrm{Im}(r_2) = \frac{-(a+b+aA)}{X\overline{X}}$$

The amplitudes ($\hat{a}_{B1}$ and $\hat{a}_{B2}$) of bays 1 and 2 are the magnitudes of the complex numbers r_1 and r_2 and the corresponding phase lags are the angles of the complex numbers:

$$\hat{a}_{B1} = \sqrt{\mathrm{Re}(r_1)^2 + \mathrm{Im}(r_1)^2} \tag{2.43}$$

$$\varepsilon_{B1} = -\tan^{-1}\left(\frac{\mathrm{Im}(r_1)}{\mathrm{Re}(r_1)}\right) \tag{2.44}$$

$$\hat{a}_{B2} = \sqrt{\mathrm{Re}(r_2)^2 + \mathrm{Im}(r_2)^2} \tag{2.45}$$

$$\varepsilon_{B2} = -\tan^{-1}\left(\frac{\mathrm{Im}(r_2)}{\mathrm{Re}(r_2)}\right) \tag{2.46}$$

The velocities u_{c1} and u_{c2} through inlets 1 and 2, respectively, are therefore given by

$$u_{c1} = u_{\max 1}\cos\left(\theta - \varepsilon_{v1}\right) \tag{2.47}$$

$$u_{c2} = u_{\max 2}\cos\left(\theta - \varepsilon_{v2}\right) \tag{2.48}$$

where u_{max1} and u_{max2} are the maximum velocities through inlets 1 and 2, respectively, ε_{v1} and ε_{v2} are the phase lags between the velocity in inlet 1 and HW or LW in the ocean, and in inlet 2 and HW or LW in the ocean.

Substituting for η_o and η_{B1} from Eqs. (2.18) and (2.34) in Eq. (2.24) and combining Eqs. (2.47) and (2.24) we get the required expression for u_{max1}. Similarly we

can obtain the expression for u_{max2}. It should be noted that velocity is out of phase with respect to displacement by $\pi/2$. Therefore, $\varepsilon_{v1} = \varepsilon_{B1} - \pi/2$ and $\varepsilon_{v2} = \varepsilon_{B2} - \pi/2$.

2.3.2 Three Inlets and Two Bays with Two Inlets Connected to Ocean

The inlet bay system is defined in Figure 2.3. In this system two bays are connected to each other with inlets 2 and inlet 3 and 1 connects bay 1 to the ocean.

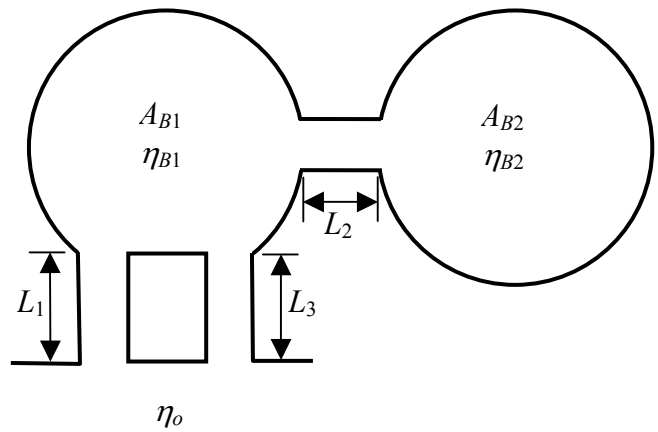

Figure 2.3 Two bays and three inlets, two inlets are connected to ocean.

The velocity in inlets 1 and 2 is given by Eq. (2.24) and Eq. (2.26) respectively. The velocity in inlet 3 is given by Eq. (2.49):

$$u_{c3} = \sqrt{\frac{2g}{a_o}} C_{DL3} \left(\eta_o - \eta_{B1} \right) \tag{2.49}$$

where u_{c3} = velocity through the inlet 3 and

$$C_{DL3} = \frac{1}{\sqrt{k_{en} + k_{ex} + \frac{fL_3}{4R_3}}} \sqrt{\frac{a_o}{\left(\eta_o - \eta_{B1} \right)_{\max}}} \tag{2.50}$$

where

L_3 = inlet 3 length, and

R_3 = hydraulic radius of inlet 3 channel.

The governing equations of continuity are

$$Q_1 + Q_3 = u_{c1}A_{c1} + u_{c3}A_{c3} = A_{B1}\frac{d\eta_{B1}}{dt} + A_{B2}\frac{d\eta_{B2}}{dt} \tag{2.51}$$

$$Q_2 = u_{c2}A_{c2} = A_{B2}\frac{d\eta_{B2}}{dt} \tag{2.52}$$

where

Q_1, Q_2, Q_3 = discharges through inlets 1, 2 and 3,

A_{c1}, A_{c2}, A_{c3} = flow cross-sectional areas at inlets 1, 2 and 3, and

A_{B1}, A_{B2} = bay water surface areas.

Substituting for the velocity expressions in the above equations we obtain

$$\eta_o - \eta_{B1} = \frac{1}{C_1 + C_3}\left[\frac{d\eta_{B1}}{dt} + \frac{A_{B2}}{A_{B1}}\frac{d\eta_{B2}}{dt}\right] \tag{2.53}$$

$$\eta_{B1} - \eta_{B2} = \frac{1}{C_2}\left[\frac{d\eta_{B2}}{dt}\right] \tag{2.54}$$

where C_1 and C_2 are expressed by Eqs. (2.31) and (2.33), and

$$C_3 = C_{DL3}\frac{A_{c3}}{A_{B1}}\sqrt{\frac{2g}{a_o}} \tag{2.55}$$

Stating Eqs. (2.53) and (2.54) in the dimensionless form we obtain

$$\hat{\eta}_o - \hat{\eta}_{B1} = \frac{\sigma}{C_1 + C_3}\left[\frac{d\hat{\eta}_{B1}}{d\theta} + \frac{A_{B2}}{A_{B1}}\frac{d\hat{\eta}_{B2}}{d\theta}\right] \tag{2.56}$$

$$\hat{\eta}_{B1} - \hat{\eta}_{B2} = \frac{\sigma}{C_2}\left[\frac{d\hat{\eta}_{B2}}{d\theta}\right] \tag{2.57}$$

where $\hat{\eta}_o$, $\hat{\eta}_{B1}$ and $\hat{\eta}_{B2}$ are defined in Eqs. (2.18), (2.34) and (2.35), respectively. The solution of the system of Eqs. (2.56) and (2.57) is given below.

1 Define the following constants

$$\frac{\sigma}{C_1+C_3}=a\,,\ \frac{\sigma}{C_2}=b\,,\ \frac{A_{B2}}{A_{B1}}=A\,,\ \hat{\eta}_o=\mathrm{Re}(e^{i\theta})$$

2 Let

$$\hat{\eta}_{B1}=\mathrm{Re}\left(e^{i(\theta-\varepsilon_{B1})}\right)=r_1\,,\ \hat{\eta}_{B2}=\mathrm{Re}\left(e^{i(\theta-\varepsilon_{B2})}\right)=r_2\,;\ \frac{d\hat{\eta}_{B1}}{d\theta}=ir_1\,,\ \frac{d\hat{\eta}_{B2}}{d\theta}=ir_2$$

3 So the equations are reduced to

$$1=(ai+1)r_1+aAir_2 \tag{2.58}$$

$$0=-r_1+(bi+1)r_2 \tag{2.59}$$

4 Solve these equations by the matrix method.

$$\begin{pmatrix}1\\0\end{pmatrix}=\begin{pmatrix}r_1\\r_2\end{pmatrix}\begin{pmatrix}ai+1 & aAi\\ -1 & bi+1\end{pmatrix} \tag{2.60}$$

5 Solving the above equations yields

$$r_1=\frac{-i\left(b-i\right)}{X} \tag{2.61}$$

$$r_2=\frac{-1}{X} \tag{2.62}$$

$$X=(ab-1)-i(aA+a+b)\,;\ \overline{X}=(ab-1)+i(aA+a+b)$$

$$X\overline{X}=(ab-1)^2+(aA+a+b)^2$$

$$\mathrm{Re}(r_1)=\frac{b\left(b+a+aA\right)-(ab-1)}{X\overline{X}}\,;\ \mathrm{Im}(r_1)=\frac{-b\left(ab-1\right)-\left(a+b+aA\right)}{X\overline{X}}$$

$$\mathrm{Re}(r_2)=\frac{-(ab-1)}{X\overline{X}}\,;\ \mathrm{Im}(r_2)=\frac{-(a+b+aA)}{X\overline{X}}$$

The amplitudes ($\hat{a}_{B1}$ and $\hat{a}_{B2}$) of bays 1 and 2 are the magnitudes of the complex numbers r_1 and r_2 and the phase lags are the corresponding angles:

$$\hat{a}_{B1} = \sqrt{\mathrm{Re}(r_1)^2 + \mathrm{Im}(r_1)^2} \tag{2.63}$$

$$\varepsilon_{B1} = -\tan^{-1}\left(\frac{\mathrm{Im}(r_1)}{\mathrm{Re}(r_1)}\right) \tag{2.64}$$

$$\hat{a}_{B2} = \sqrt{\mathrm{Re}(r_2)^2 + \mathrm{Im}(r_2)^2} \tag{2.65}$$

$$\varepsilon_{B2} = -\tan^{-1}\left(\frac{\mathrm{Im}(r_2)}{\mathrm{Re}(r_2)}\right) \tag{2.66}$$

The velocities u_{c1} and u_{c2} through inlets 1 and 2, respectively, are given by Eqs. (2.47) and (2.48), and u_{c3} through inlet 3 is obtained from

$$u_{c3} = u_{\max 3}\cos\left(\theta - \varepsilon_{v3}\right) \tag{2.67}$$

where u_{max3} is the maximum velocity through inlet 3 and ε_{v3} is the phase lag between velocity in inlet 3 and HW or LW in the ocean. Substituting for η_o and η_{B1} from Eqs. (2.18) and (2.34) into Eq. (2.49) and combining Eqs. (2.49) and (2.67) we get the required expression for u_{max3}. Then the phase lag $\varepsilon_{v3} = \varepsilon_{B1} - \pi/2$.

2.3.3 Three Inlets and Three Bays with One Inlet connected to Ocean.

This inlet bay system as defined in Figure.2.4 has three interconnected bays with inlets 2 and 4, while inlet 1 connects bay 1 to the ocean. The velocities in inlets 1 and 2 are given by Eqs. (2.24) and (2.26), respectively. The velocity in inlet 4 is given by Eq. (2.68):

$$u_{c4} = \sqrt{\frac{2g}{a_{B1}}}C_{DL4}\left(\eta_{B1} - \eta_{B3}\right) \tag{2.68}$$

where u_{c4} = velocity through the inlet 4 and

$$C_{DL4} = \frac{1}{\sqrt{k_{en} + k_{ex} + \frac{fL_4}{4R_4}}} \sqrt{\frac{a_{B1}}{(\eta_{B1} - \eta_{B3})_{\max}}}$$

with L_4 = inlet length and R_4 = hydraulic radius of inlet 4 channel.

The governing continuity equations are

$$Q_1 = u_{c1} A_{c1} = A_{B1} \frac{d\eta_{B1}}{dt} + A_{B2} \frac{d\eta_{B2}}{dt} + A_{B3} \frac{d\eta_{B3}}{dt} \tag{2.69}$$

$$Q_2 = u_{c2} A_{c2} = A_{B2} \frac{d\eta_{B2}}{dt} \tag{2.70}$$

$$Q_4 = u_{c4} A_{c4} = A_{B3} \frac{d\eta_{B3}}{dt} \tag{2.71}$$

Q_1, Q_2, Q_4 = discharges through inlets 1, 2 and 4

A_{c1}, A_{c2}, A_{c4} = flow cross-sectional areas at inlets 1, 2 and 4.

A_{B1}, A_{B2}, A_{B3} = bay water surface areas.

Substituting the velocity expressions in the above equations we obtain

$$\eta_o - \eta_{B1} = \frac{1}{C_1} \left[\frac{d\eta_{B1}}{dt} + \frac{A_{B2}}{A_{B1}} \frac{d\eta_{B2}}{dt} + \frac{A_{B3}}{A_{B1}} \frac{d\eta_{B3}}{dt} \right] \tag{2.72}$$

$$\eta_{B1} - \eta_{B2} = \frac{1}{C_2} \left[\frac{d\eta_{B2}}{dt} \right] \tag{2.73}$$

$$\eta_{B1} - \eta_{B3} = \frac{1}{C_4} \left[\frac{d\eta_{B3}}{dt} \right] \tag{2.74}$$

where C_1 and C_2 are as expressed by Eqs. (2.31) and (2.33), and

$$C_4 = C_{DL4} \frac{A_{c4}}{A_{B3}} \sqrt{\frac{2g}{a_{B1}}} \tag{2.75}$$

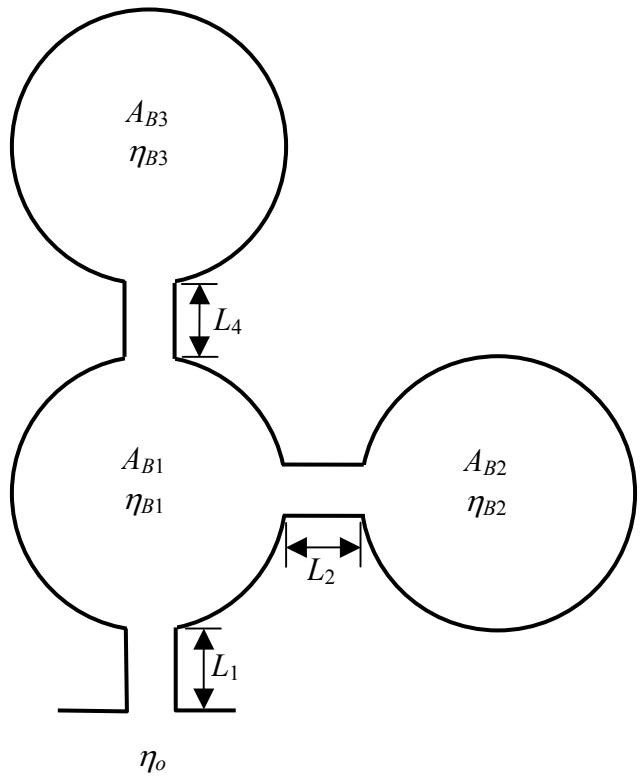

Figure 2.4 Three bays and three inlets with one inlet connecting to the ocean.

Stating the above equations in the dimensionless form the desired solution is obtained by solving the following three equations:

$$\hat{\eta}_o - \hat{\eta}_{B1} = \frac{\sigma}{C_1}\left[\frac{d\hat{\eta}_{B1}}{d\theta} + \frac{A_{B2}}{A_{B1}}\frac{d\hat{\eta}_{B2}}{d\theta} + \frac{A_{B3}}{A_{B1}}\frac{d\hat{\eta}_{B3}}{d\theta}\right] \tag{2.76}$$

$$\hat{\eta}_{B1} - \hat{\eta}_{B2} = \frac{\sigma}{C_2}\left[\frac{d\hat{\eta}_{B2}}{d\theta}\right] \tag{2.77}$$

$$\hat{\eta}_{B1} - \hat{\eta}_{B3} = \frac{\sigma}{C_4}\left[\frac{d\hat{\eta}_{B3}}{d\theta}\right] \tag{2.78}$$

where $\hat{\eta}_o$, $\hat{\eta}_{B1}$ and $\hat{\eta}_{B2}$ are defined by Eqs. (2.18), (2.34) and (2.35), respectively, and $\hat{\eta}_{B3}$ is

$$\hat{\eta}_{B3} = \hat{a}_{B3}\cos(\theta - \varepsilon_{B3}) \tag{2.79}$$

As before the above equations are solved by using complex numbers as follows:

1 Define the following constants

$$\frac{\sigma}{C_1} = a\,,\ \frac{\sigma}{C_2} = b\,,\ \frac{\sigma}{C_4} = c\,,\ \frac{A_{B2}}{A_{B1}} = A\,,\ \frac{A_{B3}}{A_{B1}} = B\,,\ \hat{\eta}_o = \mathrm{Re}(e^{i\theta})$$

2 Let

$$\hat{\eta}_{B1} = \mathrm{Re}\left(e^{i(\theta-\varepsilon_{B1})}\right) = r_1\,,\ \hat{\eta}_{B2} = \mathrm{Re}\left(e^{i(\theta-\varepsilon_{B2})}\right) = r_2\,,\ \eta_{B3} = \mathrm{Re}\left(e^{i(\theta-\varepsilon_{B3})}\right) = r_3\,,$$

$$\frac{d\hat{\eta}_{B1}}{d\theta} = ir_1\,,\ \frac{d\hat{\eta}_{B2}}{d\theta} = ir_2\,,\ \frac{d\hat{\eta}_{B3}}{d\theta} = ir_3$$

3 So the equations are reduced to

$$1 = (ai+1)r_1 + aAir_2 + aBir_3 \tag{2.80}$$

$$0 = -r_1 + (bi+1)r_2 + 0r_3 \tag{2.81}$$

$$0 = -r_1 + 0r_2 + (ci+1)r_3 \tag{2.82}$$

4 Solving the equations by matrix method:

$$\begin{pmatrix} 1 \\ 0 \\ 0 \end{pmatrix} = \begin{pmatrix} r_1 \\ r_2 \\ r_3 \end{pmatrix} \begin{pmatrix} ai+1 & aAi & aBi \\ -1 & bi+1 & 0 \\ -1 & 0 & ci+1 \end{pmatrix} \tag{2.83}$$

yields

$$r_1 = \frac{(c-i)(b-i)}{X} \tag{2.84}$$

$$r_2 = \frac{-i(c-i)}{X} \tag{2.85}$$

$$r_3 = \frac{-i(b-i)}{X} \tag{2.86}$$

$$X = (ac+ab+bc+aBb+aAc-1) + i(-aA+abc-a-b-c-aB)$$

$$\overline{X} = (ac+ab+bc+aBb+aAc-1) - i(-aA+abc-a-b-c-aB)$$

$$X\overline{X} = (ac+ab+bc+aBb+aAc-1)^2 + (-aA+abc-a-b-c-aB)^2$$

$$\mathrm{Re}(r_1) = \frac{b^2\left(1+aBc+c^2\right)+c^2\left(1+aAb\right)+a\left(bA+Bc\right)+1}{X\overline{X}}$$

$$\mathrm{Im}(r_1) = \frac{-a\left(1+A+B+b^2+c^2+b^2c^2+Bbc+Ac^2+Bb^2-bcB\right)}{X\overline{X}}$$

$$\mathrm{Re}(r_2) = \frac{-ab-aBb+aBc+1+c^2-abc^2}{X\overline{X}}$$

$$\mathrm{Im}(r_2) = \frac{-(a+b+aA+aB+aBbc+ac^2+bc^2+aAc^2)}{X\overline{X}}$$

$$\mathrm{Re}(r_3) = \frac{-ac-aAc+abA-ab^2c+b^2+1}{X\overline{X}}$$

$$\mathrm{Im}(r_3) = \frac{-(a+c+aA+aB+abcA+ab^2+cb^2+aBb^2)}{X\overline{X}}$$

The amplitudes ($\hat{a}_{B1}$, $\hat{a}_{B2}$ and $\hat{a}_{B3}$) of bay1, bays 2 and 3 are the magnitudes of the complex numbers r_1, r_2 and r_3, and the corresponding phase lags are the angles of the complex numbers:

$$\hat{a}_{B1} = \sqrt{\mathrm{Re}(r_1)^2 + \mathrm{Im}(r_1)^2} \tag{2.87}$$

$$\varepsilon_{B1} = -\tan^{-1}\left(\frac{\mathrm{Im}(r_1)}{\mathrm{Re}(r_1)}\right) \tag{2.88}$$

$$\hat{a}_{B2} = \sqrt{\mathrm{Re}(r_2)^2 + \mathrm{Im}(r_2)^2} \tag{2.89}$$

$$\varepsilon_{B2} = -\tan^{-1}\left(\frac{\mathrm{Im}(r_2)}{\mathrm{Re}(r_2)}\right) \tag{2.90}$$

$$\hat{a}_{B3} = \sqrt{\mathrm{Re}(r_3)^2 + \mathrm{Im}(r_3)^2} \tag{2.91}$$

$$\varepsilon_{B3} = -\tan^{-1}\left(\frac{\mathrm{Im}(r_3)}{\mathrm{Re}(r_3)}\right) \tag{2.92}$$

The velocities u_{c1} and u_{c2} through inlets 1 and 2, respectively, are given by Eqs. (2.47) and (2.48), and u_{c4} through inlet 4 is given by

$$u_{c4} = u_{\max 4} \cos\left(\theta - \varepsilon_{v4}\right) \tag{2.93}$$

where u_{max4} is the maximum velocity through inlet 4 and ε_{v4} is the corresponding phase lags between this velocity and HW or LW in the ocean. Substituting for η_{B1} and η_{B3} from Eqs. (2.34) and (2.79)into Eq. (2.68) and combining Eqs. (2.93) and (2.68) we get the desired expression for u_{max4}. Phase lag $\varepsilon_{v4} = \varepsilon_{B3} - \pi/2$.

2.3.4 Four Inlets and Three Bays with Two Inlets Connected to Ocean.

This system as defined in Figure 2.5 has three interconnected bays with inlets 2 and 4, while and inlets 1 and 3 connect bay 1 to the ocean. The velocities in inlets 1, 2, 3 and 4 are given by Eqs. (2.24), (2.26), (2.49) and (2.68), respectively.

The governing continuity equations are written as follows.

$$Q_1 + Q_3 = u_{c1}A_{c1} + u_{c3}A_{c3} = A_{B1}\frac{d\eta_{B1}}{dt} + A_{B2}\frac{d\eta_{B2}}{dt} + A_{B3}\frac{d\eta_{B3}}{dt} \tag{2.94}$$

$$Q_2 = u_{c2}A_{c2} = A_{B2}\frac{d\eta_{B2}}{dt} \tag{2.95}$$

$$Q_4 = u_{c4}A_{c4} = A_{B3}\frac{d\eta_{B3}}{dt} \tag{2.96}$$

Next, substituting the velocity expressions in the above equations yields

$$\eta_o - \eta_{B1} = \frac{1}{C_1 + C_3}\left[\frac{d\eta_{B1}}{dt} + \frac{A_{B2}}{A_{B1}}\frac{d\eta_{B2}}{dt} + \frac{A_{B3}}{A_{B1}}\frac{d\eta_{B3}}{dt}\right] \tag{2.97}$$

$$\eta_{B1} - \eta_{B2} = \frac{1}{C_2}\left[\frac{d\eta_{B2}}{dt}\right] \tag{2.98}$$

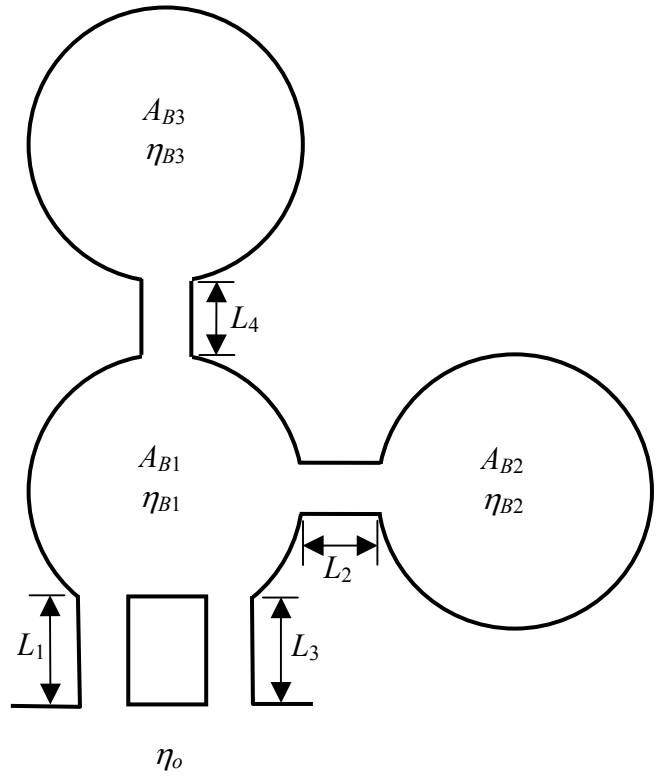

Figure 2.5 Three bays and four inlets, two inlets connect to ocean.

$$\eta_{B1} - \eta_{B3} = \frac{1}{C_4}\left[\frac{d\eta_{B3}}{dt}\right] \tag{2.99}$$

where C_1, C_2, C_3 and C_4 are as expressed by Eqs. (2.31), (2.33), (2.55) and (2.75), respectively.

Now we may state the above equations in the dimensionless form as

$$\hat{\eta}_o - \hat{\eta}_{B1} = \frac{\sigma}{C_1 + C_3}\left[\frac{d\hat{\eta}_{B1}}{d\theta} + \frac{A_{B2}}{A_{B1}}\frac{d\hat{\eta}_{B2}}{d\theta} + \frac{A_{B3}}{A_{B1}}\frac{d\hat{\eta}_{B3}}{d\theta}\right] \tag{2.100}$$

$$\hat{\eta}_{B1} - \hat{\eta}_{B2} = \frac{\sigma}{C_2}\left[\frac{d\hat{\eta}_{B2}}{d\theta}\right] \tag{2.101}$$

$$\hat{\eta}_{B1} - \hat{\eta}_{B3} = \frac{\sigma}{C_4}\left[\frac{d\hat{\eta}_{B3}}{d\theta}\right] \tag{2.102}$$

where $\hat{\eta}_o$, $\hat{\eta}_{B1}$, $\hat{\eta}_{B2}$ and $\hat{\eta}_{B3}$ are defined by Eqs. (2.18), (2.34), (2.35) and (2.79), respectively. These equations are solved as follows:

1 Define the following constants

$$\frac{\sigma}{C_1+C_3}=a\,,\ \frac{\sigma}{C_2}=b\,,\ \frac{\sigma}{C_4}=c\,,\ \frac{A_{B2}}{A_{B1}}=A\,,\ \frac{A_{B3}}{A_{B1}}=B\,,\ \hat{\eta}_o=\mathrm{Re}(e^{i\theta})$$

2 Let

$$\hat{\eta}_{B1}=\mathrm{Re}\left(e^{i(\theta-\varepsilon_{B1})}\right)=r_1\,,\ \hat{\eta}_{B2}=\mathrm{Re}\left(e^{i(\theta-\varepsilon_{B2})}\right)=r_2\,,\ \eta_{B3}=\mathrm{Re}\left(e^{i(\theta-\varepsilon_{B3})}\right)=r_3\,,$$

$$\frac{d\hat{\eta}_{B1}}{d\theta}=ir_1\,,\ \frac{d\hat{\eta}_{B2}}{d\theta}=ir_2\,,\ \frac{d\hat{\eta}_{B3}}{d\theta}=ir_3$$

3 So the equations are reduced to

$$1=(ai+1)r_1+aAir_2+aBir_3 \tag{2.103}$$

$$0=-r_1+(bi+1)r_2+0r_3 \tag{2.104}$$

$$0=-r_1+0r_2+(ci+1)r_3 \tag{2.105}$$

4 Solve these equations by matrix method:

$$\begin{pmatrix}1\\0\\0\end{pmatrix}=\begin{pmatrix}r_1\\r_2\\r_3\end{pmatrix}\begin{pmatrix}ai+1 & aAi & aBi\\ -1 & bi+1 & 0\\ -1 & 0 & ci+1\end{pmatrix} \tag{2.106}$$

5 Thus we obtain

$$r_1=\frac{(c-i)(b-i)}{X} \tag{2.107}$$

$$r_2=\frac{-i(c-i)}{X} \tag{2.108}$$

$$r_3=\frac{-i(b-i)}{X} \tag{2.109}$$

$$X=(ac+ab+bc+aBb+aAc-1)+i(-aA+abc-a-b-c-aB)$$

$$\overline{X}=(ac+ab+bc+aBb+aAc-1)-i(-aA+abc-a-b-c-aB)$$

$$X\overline{X} = (ac + ab + bc + aBb + aAc - 1)^2 + (-aA + abc - a - b - c - aB)^2$$

$$\mathrm{Re}(r_1) = \frac{b^2\left(1 + aBc + c^2\right) + c^2\left(1 + aAb\right) + a\left(bA + Bc\right) + 1}{X\overline{X}}$$

$$\mathrm{Im}(r_1) = \frac{-a\left(1 + A + B + b^2 + c^2 + b^2c^2 + Bbc + Ac^2 + Bb^2 - bcB\right)}{X\overline{X}}$$

$$\mathrm{Re}(r_2) = \frac{-ab - aBb + aBc + 1 + c^2 - abc^2}{X\overline{X}}$$

$$\mathrm{Im}(r_2) = \frac{-(a + b + aA + aB + aBbc + ac^2 + bc^2 + aAc^2)}{X\overline{X}}$$

$$\mathrm{Re}(r_3) = \frac{-ac - aAc + abA - ab^2c + b^2 + 1}{X\overline{X}}$$

$$\mathrm{Im}(r_3) = \frac{-(a + c + aA + aB + abcA + ab^2 + cb^2 + aBb^2)}{X\overline{X}}$$

The amplitudes ($\hat{a}_{B1}$, $\hat{a}_{B2}$ and $\hat{a}_{B3}$) of bays1, 2 and 3 are the magnitudes of the complex numbers r_1, r_2 and r_3, and the corresponding phase lags are the angles of the complex numbers:

$$\hat{a}_{B1} = \sqrt{\mathrm{Re}(r_1)^2 + \mathrm{Im}(r_1)^2} \tag{2.110}$$

$$\varepsilon_{B1} = -\tan^{-1}\left(\frac{\mathrm{Im}(r_1)}{\mathrm{Re}(r_1)}\right) \tag{2.111}$$

$$\hat{a}_{B2} = \sqrt{\mathrm{Re}(r_2)^2 + \mathrm{Im}(r_2)^2} \tag{2.112}$$

$$\varepsilon_{B2} = -\tan^{-1}\left(\frac{\mathrm{Im}(r_2)}{\mathrm{Re}(r_2)}\right) \tag{2.113}$$

$$\hat{a}_{B3} = \sqrt{\mathrm{Re}(r_3)^2 + \mathrm{Im}(r_3)^2} \tag{2.114}$$

$$\varepsilon_{B3} = -\tan^{-1}\left(\frac{\mathrm{Im}(r_3)}{\mathrm{Re}(r_3)}\right) \tag{2.115}$$

Then the velocities u_{c1}, u_{c2}, u_{c3} and u_{c4} are given by Eqs. (2.47), (2.48), (2.67) and (2.93), respectively.

CHAPTER 3
STABILITY OF MULTIPLE INLET-BAY SYSTEMS

3.1 Stability Problem Definition

An inlet is considered stable when after a small change the cross-sectional area returns to its equilibrium value. Each inlet is subject to two opposing forces, the waves on one hand, which tend to push sand into the inlet, and the tidal current on the other hand, which tries to carry sand out of the channel back to the sea or the bay. The size of the inlet and its stability are determined by the relative strengths of these two opposing forces.

3.2 Stability Criteria

Inlet stability as considered here basically deals with the equilibrium between the inlet cross-section area and the hydraulic environment. The pertinent parameters are the actual tide-maximum bottom shear stress $\hat{\tau}$ and the equilibrium shear stress $\hat{\tau}_{eq}$. The equilibrium shear stress is defined as the bottom stress induced by the tidal current required to flush-out sediment carried into the inlet. When $\hat{\tau}$ equals $\hat{\tau}_{eq}$ the inlet is considered to be in equilibrium. When $\hat{\tau}$ is larger than $\hat{\tau}_{eq}$ the inlet is in the scouring mode, and when $\hat{\tau}$ is smaller $\hat{\tau}_{eq}$ the inlet is in the shoaling mode. The value of equilibrium shear stress depends on the waves and associated littoral drift and sediment. Considering inlets at equilibrium on various coasts, Bruun (1978) found the value of equilibrium stress in fairly narrow range:

$$3.5Pa < \hat{\tau}_{eq} < 5.5Pa$$

The value of actual shear stress is obtained from

$$\tau = \rho F u_{\max} \, | u_{\max} | \tag{3.1}$$

where F is the friction coefficient, a function of bottom roughness, k, u_{max} is the maximum tidal velocity in the inlet, a function of area and length of the inlet, as discussed in Chapter 2 and ρ is the fluid density. Therefore, $\hat{\tau}$ can be written as a function of following form

$$\hat{\tau} = f(A, L, k, m)$$

where m is the sum of entrance and exit losses. The plotted function $\hat{\tau}(A)$ is called a closure curve, as shown in Figure 3.1. It is clear from the calculation shown in the Appendix B that $\hat{\tau}$ is a strong function of A and a weak function of L, m, k. The strong dependence of $\hat{\tau}$ on A explains why inlets adjust to changes in the hydraulic environment primarily via a change in the cross-sectional area.

3.2.1 Stability Analysis for One-Inlet Bay System

Making use of the Escoffier (1940) diagram, Figure 3.2, one can study the response of the inlet to change in area. In the Figure, A_I and A_{II} both represent equilibrium flow areas, with A_I representing *unstable* equilibrium and A_{II} representing *stable* equilibrium. If the inlet cross-sectional area A were reduced but remained larger than A_I, the actual shear stress would be larger than the equilibrium shear stress and A would return to the value A_{II}. If the cross-sectional area were reduced below A_I, the shear stress would become lower than its equilibrium value and the inlet would close. If A became larger than A_{II}, the actual shear stress would become larger than equilibrium value and A would return to A_{II}. Note that the equilibrium condition only exists if the line $\hat{\tau}=\hat{\tau}_{eq}$ intersects the closure curve $\hat{\tau}=\hat{\tau}(A)$.

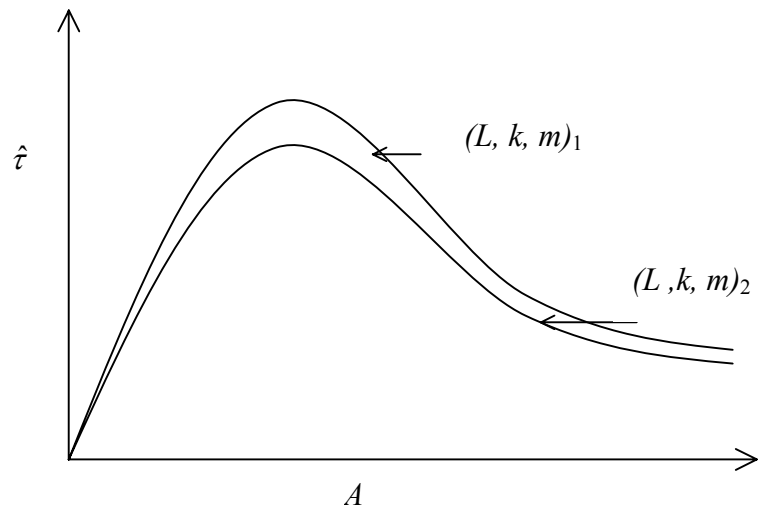

Figure 3.1 Closure curves (source: van de Kreeke, 1985)

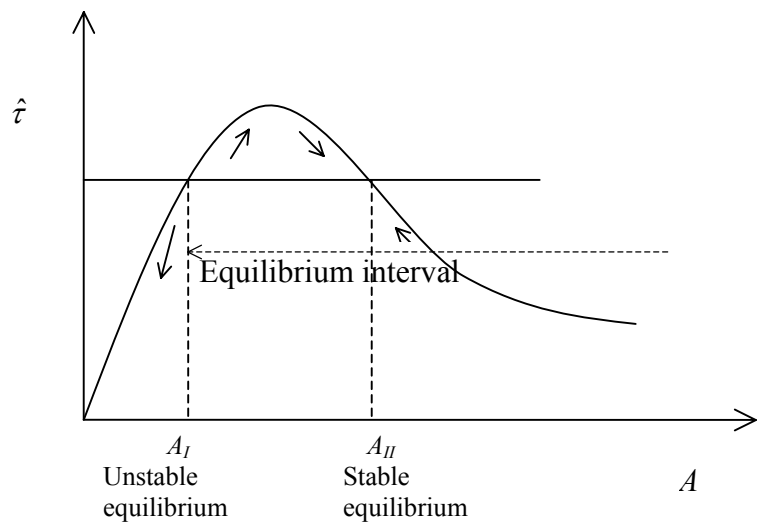

Figure 3.2 Escoffier diagram (source: van de Kreeke, 1985)

The equilibrium interval for the stable cross-section, A_{II}, ranges from A_I to infinity.

3.2.2 Stability of Two Inlets in a Bay

Similar to a single inlet, it can be shown that shear stresses $\hat{\tau}_1$ and $\hat{\tau}_2$ for two inlets in a bay strongly depend on A_1 and A_2 and are weak functions of (L_1, k_1, m_1, L_2, k_2, m_2). The functions $\hat{\tau}_1(A_1, A_2)$ and $\hat{\tau}_2(A_1, A_2)$ are referred to as a closure surfaces. The shape of $\hat{\tau}_2(A_1, A_2)$ is qualitatively illustrated in Figure 3.3. For a constant A_1, the curve $\hat{\tau}_1(A_1)$ is similar to the closure curve shown in Figure 3.1. The value of $\hat{\tau}_2$ decreases with increasing A_1.

With the help of a closure surface in Figure 3.3, the loci of (A_1, A_2) for which $\hat{\tau}_2 = \hat{\tau}_{eq}$, $\hat{\tau}_2 = \hat{\tau}_{eq} + 1$, $\hat{\tau}_2 = \hat{\tau}_{eq} - 1$ are plotted in Figure 3.4. The locus of $\hat{\tau}_2 = \hat{\tau}_{eq}$ is referred to as the equilibrium flow curve for Inlet 2. Using the same reasoning as for a single inlet and assuming that the cross-sectional area of Inlet 1 is constant, it follows that if $A_2 = A_I$, Inlet 2 will shoal and close; if $A_2 = A_{II}$, Inlet 2 will scour until the cross-sectional area attains a value A_s, and if $A_2 = A_{III}$, Inlet 2 will shoal until the cross-sectional area attains the value A_s.

The locus of (A_1, A_2) for which Inlet 2 has a stable equilibrium flow area is the enhanced (by a thicker line) part of the equilibrium flow curve for Inlet 2. Similarly, the locus of (A_1, A_2) for which Inlet 1 has a stable equilibrium flow area is the enhanced part of the equilibrium flow curve for Inlet 1. The condition for the existence of stable equilibrium flow areas for both Inlet 1 and Inlet 2 is that the enhanced parts of the equilibrium flow curves intersect. The common equilibrium interval of the two is

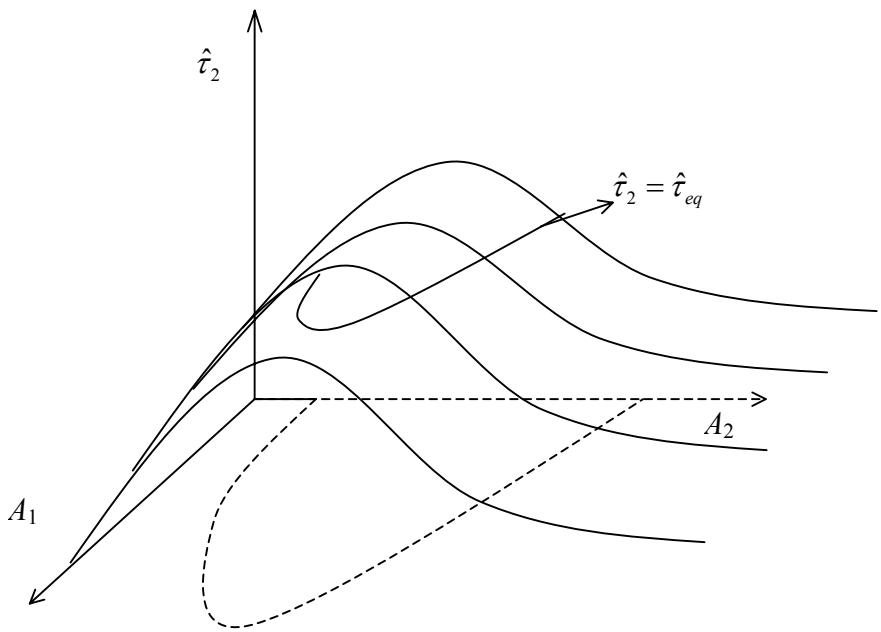

Figure 3.3 Closure surfaces (source: van de Kreeke, 1985)

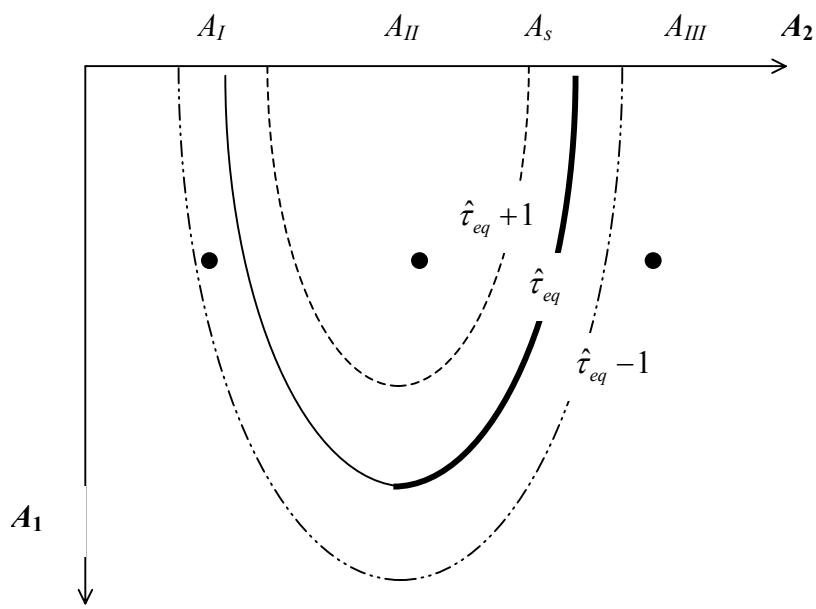

Figure 3.4 Equilibrium flow curve for Inlet 2 (source: van de Kreeke, 1985)

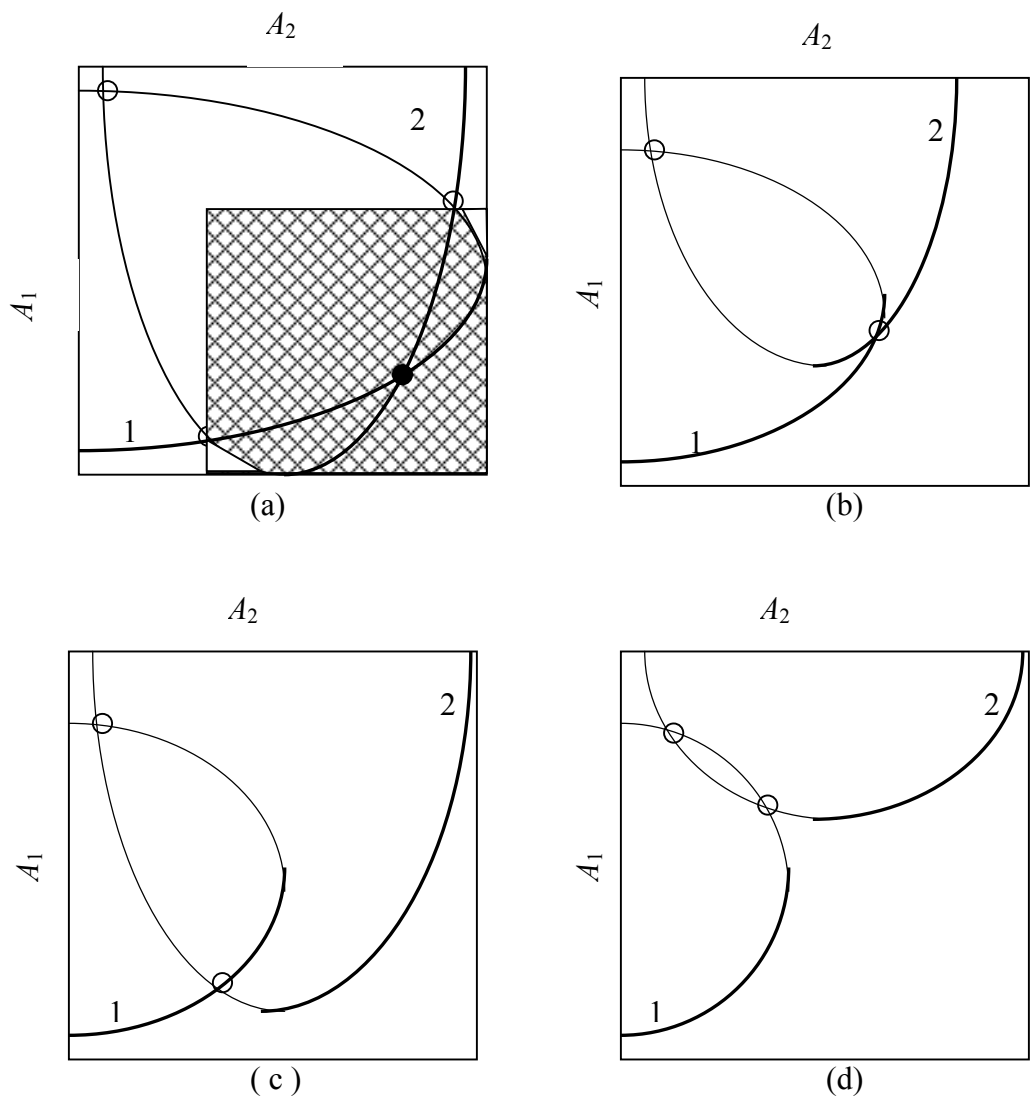

Figure 3.5 Possible configurations of equilibrium flow curves for a two-inlet bay system. Stable equilibrium flow area is represented by ● and unstable equilibrium is represented by ○. The hatched area in (a) represents the domain of the stable equilibrium flow area (source: van de Kreeke, 1990)

represented by the hatched rectangle in Figure 3.5 (a). The general shapes of the equilibrium flow curves and their relative positions in the (A_1, A_2) plane are presented in Figure 3.5. The detailed explanations to the Figure 3.5 are given in Appendix D.

3.3 Stability Analysis with the Linearized Model

Due to the complex nature of sediment transport by waves and currents it is difficult to carry out an accurate analysis of the stability of single or multiple inlet

systems. We will therefore attempt to carry out an approximate analysis based on the van de Kreeke (1990) linearized lumped parameter model.

The justification for use of simple model is that for purpose of this study the stability analysis serves to illustrate a concept rather than to provide exact numerical results. Accurate numerical values can only be obtained by using a full-fledged two-dimension tidal model to describe the hydrodynamics of the bay.

3.3.1 Linearized lumped parameter model for *N* Inlets in a Bay

The basic assumptions of the Linearized lumped parameter model are as follows:

1 The linearized model assumes that the ocean tide and the velocity are simple harmonic functions.

2 The water level in the bay fluctuates uniformly and the bay surface area remains constant.

3 Hydrostatic pressure, and shear stress distribution along the wetted perimeter of the inlet cross-section is uniform.

4 For a given bay area and inlet characteristics, the tidal amplitude and/or tidal frequency must be sufficiently large for equilibrium to exist. Similarly, larger the littoral drift due to waves, larger the equilibrium shear stress required to balance it and therefore the equilibrium velocity, the larger the required bay surface area, tidal amplitude and the tidal frequency or, in other words, Eq. (3.17) and Eq. (3.19) must be satisfied for the existence of equilibrium areas.

5 There is no fresh water discharge in the bays.

6 In a shallow bay the effect of dissipation of tidal energy cannot be ignored, especially if the bay is large.

Inlet flow dynamics of the flow in the inlets are governed by the longitudinal pressure gradient and the bottom shear stress, van de Kreeke (1967),

$$0 = -\frac{1}{\rho}\frac{\partial p}{\partial x} - \frac{\tau}{\rho h} \tag{3.2}$$

in which p is the pressure, ρ *is* the water density, h is the depth and τ is the bottom shear stress. This stress is related to the depth mean velocity u

$$\tau = \rho F u \,|\, u \,| \tag{3.3}$$

where $F = f/8$, is the friction coefficient. Integration of Eq. (3.2) (with respect to the longitudinal x-coordinate) between the ocean and the bay yields (van de Kreeke 1988).

$$u_i \,|\, u_i \,| = \frac{2gR_i}{m_i R_i + 2F_i L_i}\left(\eta_o - \eta_B\right) \tag{3.4}$$

In Eq. (3.4), u_i refers to the cross-sectional mean velocity of the ith inlet, g is the acceleration due to gravity, m_i is the sum of exit and entrance losses, R_i is the hydraulic radius of the inlet, L_i is the length of the inlet, η_o is the ocean tide, and η_B is the bay tide. The velocity u_i is positive when going from ocean to bay.

Assuming the bay surface area to fluctuate uniformly, flow continuity can be expressed as

$$\sum_{i=1}^{N} u_i A_i = A_B \frac{d\eta_B}{dt} \tag{3.5}$$

in which A_i is the cross-sectional area, A_B is the bay surface area and t is time.

Considering u_i to be a simple harmonic function of t, Eq. (3.4) is linearized as shown in Appendix B to yield

$$\frac{8}{3\pi} u_{\max i} u_i = \frac{2gR_i}{m_i R_i + 2F_i L_i}(\eta_o - \eta_B) \tag{3.6}$$

in which u_{maxi} is the amplitude of the current velocity in the ith inlet. It follows from Eq. (3.5) and Eq. (3.6) that for a simple harmonic ocean tide (in complex notation)

$$\eta_o(t) = a_o e^{j\sigma t} \tag{3.7}$$

and assuming A_i and A_B to be constant, we obtain

$$u_i = u_{\max i} e^{j(\sigma t + \varepsilon_v)} \tag{3.8}$$

where the phase angle ε_v is considered to be the same for all inlets. Differentiating Eq. (3.6) with respect to t, eliminating $d\eta_B/dt$ between Eq. (3.5) and Eq. (3.6), and making use of the expressions for u_i and η_o yields an equation for u_i and ε_v

$$\sum_{i=1}^{N} u_{\max i} A_i + \frac{1}{2g}\frac{8}{3\pi} A_B B_i u^2{}_{\max i} j\sigma = A_B a_o j\sigma e^{-j\varepsilon_v} \tag{3.9}$$

in which the dimensionless resistance factor B_i is defined as

$$B_i = \left[\frac{R_i}{m_i R_i + 2F_i L_i}\right]^{-1} \tag{3.10}$$

where B_i is the function of A_i. Now, equating the real and imaginary parts of Eq. (3.9) and eliminating the phase angle ε_v yields the equation for u_{maxi}

$$\left[\frac{1}{2g}\right]^2 \left[\frac{8}{3\pi}\right]^2 \left[A_B\sigma\right]^2 B_i^2 u_{\max i}^4 = \left[A_B a_o \sigma\right]^2 - \left[\sum_{i=1}^{N} u_{\max i} A_i\right]^2 \tag{3.11}$$

For equilibrium flow $\hat{\tau}_i = \hat{\tau}_{eqi}$. Using linearized version in Eq. (3.6) and Eq. (3.3), the equilibrium velocity can be written as

$$u_{eqi} = \sqrt{\frac{\tau_{eqi}}{8/3\pi\rho F_i}} \tag{3.12}$$

where the approximate value of $\hat{\tau}_{eqi}$ can be taken from Mehta and Christensen (1983). For equilibrium flow areas $u_{\max i} = u_{\max eqi}$, substituting this value Eq. (3.11) becomes:

$$\left[\frac{1}{2g}\right]^2 \left[\frac{8}{3\pi}\right]^2 \left[A_B\sigma\right]^2 B_i^2 u_{\max eqi}^4 = \left[A_B a_o \sigma\right]^2 - \left[\sum_{i=1}^{N} u_{\max eqi} A_i\right]^2 \tag{3.13}$$

When the maximum tidal velocity in all the inlets equals the corresponding equilibrium value, i.e., $u_{\max i} = u_{\max eq.i}$ for i =1,2……..N, the difference between the bay and the ocean tides becomes constant. So from Eq. (3.4) it follows that

$$B_1 u^2{}_{\max eq1} = B_2 u^2{}_{\max eq2} \ldots\ldots = B_i u^2{}_{\max eqi} = B_N u^2{}_{\max eqN} \tag{3.14}$$

Eq. (3.13) and Eq. (3.14) constitute a set of N simultaneous equations with N unknowns [A_1, A_2...,A_N]. In general, more than one set of equilibrium flow areas [A_1, A_2...,A_N] will satisfy these equations. Since the dimensionless resistance factor B_i is a function of A_i. Therefore, whether for a given ocean tide (a_o, σ) and bay surface area (A_B), Eq. (3.13) and Eq. (3.14) yield sets of solutions [A_1, A_2....A_N] that are real and positive depends on the particular form of $R_i=f(A_i)$.

The function $R_i=f(A_i)$ plays an important role in the hydrodynamic efficiency of an inlet. For a given head difference, exit and entrance loss coefficients, friction factor and inlet length, the maximum tidal velocity increases with the increasing value of R, see Eq. (3.4). Therefore, larger the value of R, for a given value of A, larger the discharge. For a rectangular channel, $R_i = \frac{A_i}{W_i}$, and for triangular channel $R_i = a_i\sqrt{A_i}$ (See Appendix B).

Analytical solutions to equation Eq. (3.13) and Eq. (3.14) can be found by restricting attention to the friction-dominated flow in the inlets, i.e. m=0

From Eq. (3.10) with m = 0, we obtain

$$B_i = \frac{2F_i L_i}{R_i} \tag{3.15}$$

For rectangular inlets, substituting $R_i = \frac{A_i}{W_i}$ in Eq. (3.15) and then in Eq. (3.13) and Eq. (3.14) we get

$$\frac{A_i^2}{\left(F_i L_i W_i u^2{}_{eqi}\right)^2} = \frac{\left(A_B a_o \sigma\right)^2 \pm \sqrt{\left(A_B a_o \sigma\right)^4 - 4\left(\frac{8}{3\pi}\right)^2 \left(\frac{1}{2g}\right)^2 \left(A_B \sigma\right)^2 \left(F_1 L_1 W_1 u^3{}_{eq1} + \ldots + F_N L_N W_N u^3{}_{eqN}\right)^2}}{2\left(F_1 L_1 W_1 u^3{}_{eq1} + \ldots + F_N L_N W_N u^3{}_{eqN}\right)^2} \tag{3.16}$$

When any A_i (from Eq. (3.16)) is known, the cross-sectional areas of the other inlets follow from Eq. (3.14), with B_i given by Eq. (3.15), provided that

$$A_B \sigma a^2{}_o > 2\left(\frac{8}{3\pi}\right)\left(\frac{1}{g}\right)\left(F_1 L_1 W_1 u^3{}_{eq1} + \ldots + F_N L_N W_N u^3{}_{eqN}\right) \tag{3.17}$$

This is a quadratic equation in A_i^2 for which we have two sets of real and positive roots and two sets of complex roots.

For the triangular cross-section, $R_i = a_i \sqrt{A_i}$, substituting this in Eq. (3.13) and Eq. (3.14) we get,

$$\left[u_{eq1}\left[\frac{F_1 L_1 a_i}{F_i L_i a_1}\right]^2 + \ldots. + u_{eqN}\left[\frac{F_N L_N a_i}{F_i L_i a_N}\right]^2\right] A_i^3 - \left(A_B a_o \sigma\right)^2 A_i + \left(\frac{8}{3\pi}\right)^2 \left(A_B \sigma\right)^2 \left[\frac{F_i L_i}{a_i g}\right]^2 u_{eq_i}^4 = 0 \tag{3.18}$$

in which sets of A_i are given by Eq. (3.18) (as we have two real and positive solution for A_i). When any A_i is known, the cross-sectional areas of the other (N-1) inlets follow from Eq. (3.14) with B_i given by Eq. (3.15). One root of Eq. (3.18) is always negative. The other two are real and positive roots provided that

$$A_B \sigma a^3{}_o > \frac{3\sqrt{3}}{2}\left(\frac{8}{3\pi}\right)^2 \left[u_{1eq}^5 \left(\frac{F_1 L_1}{a_1 g}\right)^2 + \ldots.. u_{Neq}^5 \left(\frac{F_N L_N}{a_N g}\right)^2\right] \tag{3.19}$$

The above stability concept, when applied to a multiple-bay inlet system, becomes complicated because the loci of the set of the values [A_1, A_2....A_N] for which the tidal maximum of the bottom shear stress equals the equilibrium stress, are rather complicated surfaces and make it difficult to determine whether inlets are in a scouring mode or shoaling mode. With some simplifying assumptions, the stability analysis for a multiple-inlet system can be reduced to that for a two-inlet system. This is considered next in the context of the St. Andrew Bay system.

3.4 Application to St. Andrew Bay System

In the above model if N=2, the model can be applied to the two inlet system. The equilibrium flow curves for Inlet 1 and Inlet 2 are calculated from Eq. (3.11) with $u=u_{eq}$. The equilibrium flow areas are given by the solution of Eq. (3.16) for rectangular inlet and Eq. (3.18) for triangular cross-section. Figure 3.6 illustrates the equilibrium flow curve. A line can be drawn passing from the intersection of two equilibrium flow areas. Above the line $B_1>B_2$ and therefore $u_1<u_2$. Figure 3.6 can be elaborated as follows:

1. When the point defined by the actual cross-sectional areas [A_1, A_2] is located in the vertically hatched zone or anywhere outside the curves, (Zone-1), both inlets close.
2. When the point is located in the crosshatched zone, (Zone-2), Inlet 1 will remain open and Inlet 2 will close.
3. When the point is located in the diagonally hatched zone, (Zone-3), Inlet 1 will close and Inlet 2 will remain open.
4. Finally, when the point is located in the blank zone, (Zone-4), one inlet will close and the other will remain open. However, in this case which one closes depends on the relative rates of scouring and or/shoaling.

The St. Andrew Bay system is similar to the case of two inlets in a bay. In reality there are three interconnected bays, but only one is connected with the Gulf. So there is no forcing due to ocean tide from the other two bays. Thus, all the bays collectively behave as if there is only one bay connected by two inlets. So the linear model for N inlets can be applied to the St. Andrew system, where $N = 2$. The development of equilibrium curves for this case is discussed in Chapter 5.

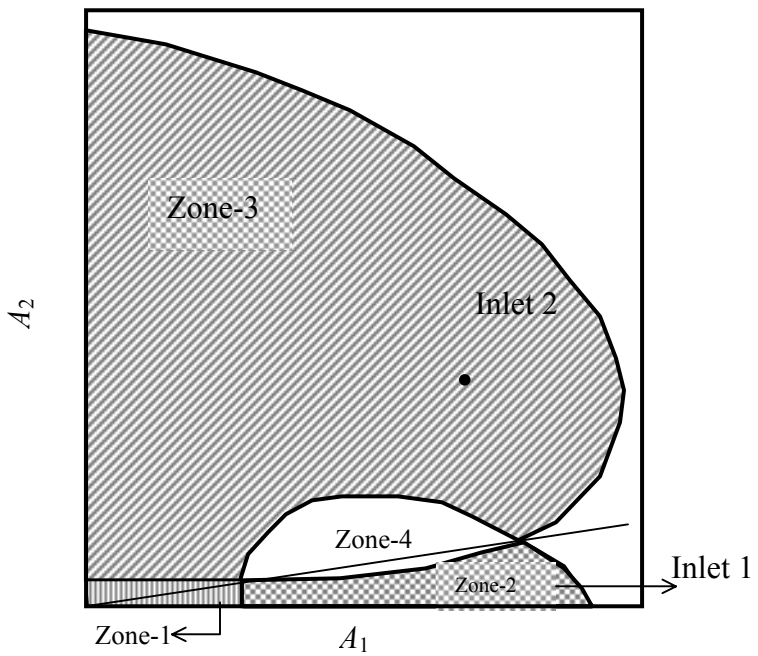

Figure 3.6 Equilibrium flow curves for two inlets in a bay (source: van de Kreeke, 1990)

CHAPTER 4
APPLICATION TO ST. ANDREW BAY COMPLEX AND ENTRANCES

4.1 Description of Study Area

St. Andrew Bay is located in Bay County on the Gulf of Mexico coast of Florida's panhandle. It is part of a three-bay and two-inlet complex. One of these inlets is St. Andrew Bay Entrance and the other is East Pass, which are connected to St. Andrew Bay on one side and the Gulf on the other. The other two bays are West Bay and the East Bay, which connect to St. Andrew Bay, as shown in the Figure 4.1 Note that West Bay as shown also includes a portion called North Bay. Prior to 1934, East Pass was the natural connection between St. Andrew Bay and the Gulf. In 1934, St. Andrew Bay Entrance (Figure. 4.2) was constructed 11 km west of East Pass through the barrier island by the federal government to provide a direct access between the Gulf and Panama City. The entrance has since been maintained by the U.S Army Corps of Engineers (USACE), Mobile District. The St. Andrew Bay State Recreational Area is located on both sides of this entrance, which has two jetties 430 m apart to prevent the closure of the inlet.

The interior shoreline of the entrance has continually eroded since it's opening. An environmentally sensitive fresh water lake located in the St. Andrew Bay State Recreational Area is vulnerable to the shoreline erosion and USACE has placed dredged soil to mitigate shoreline erosion.

East Pass finally closed in the 1998, due to the long-term effect of the opening of St. Andrew Entrance. In December 2001, a new East Pass was opened (Figure 4.3), and the effect of this new inlet is presently being monitored over the entire system.

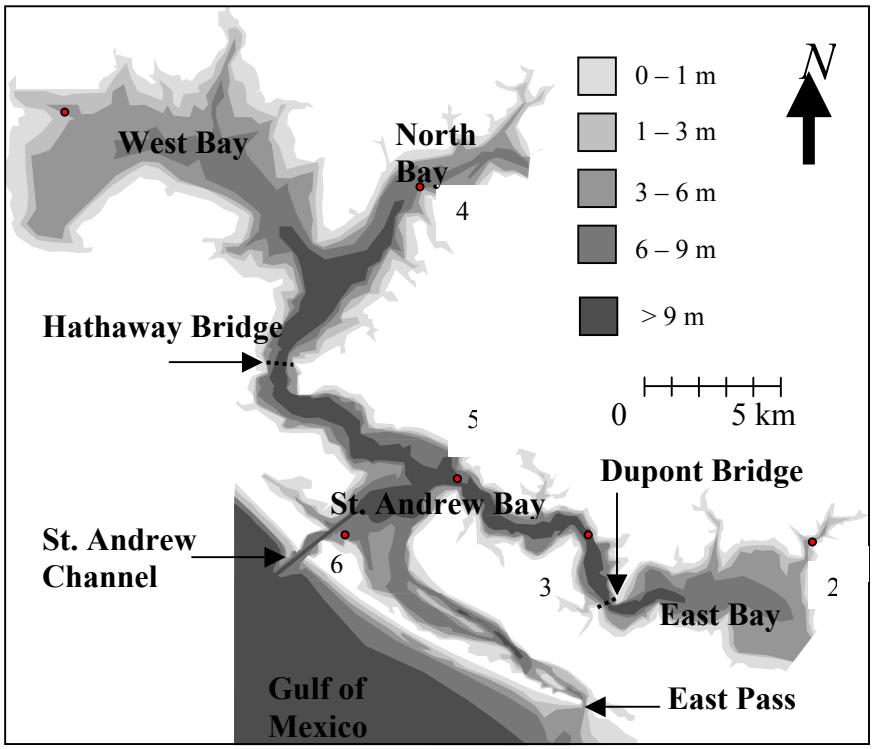

Figure 4.1 Map showing the three bays and two inlets and bathymetry of the study area. Dots show location of tide stations.

Figure 4.2 Aerial view of St. Andrew Bay Entrance in 1993. Jetties are ~430 m apart.

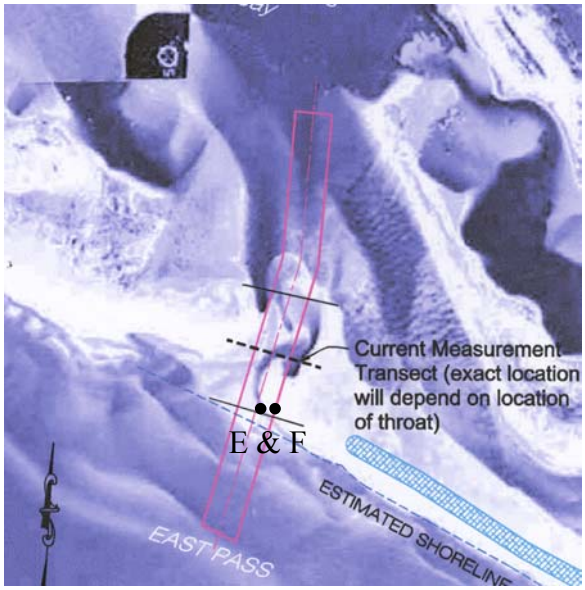

Figure 4.3 East Pass channel before it's opening in December 2001. Plan view (pre-construction) design geometry and then anticipated current measurement transects are shown. The dots show the new cross-section (source: Jain et al., 2002)

4.2 Summary of Field Data

Three hydrographic surveys were done by the University of Florida's Department of Civil and Coastal Engineering in the years 2001 and 2002. Figure 4.4 shows the bathymetry of St. Andrew Bay Entrance and the different cross-sections measured during the surveys. Cross-sections A-1, A-2 and B-1, B-2 were measured in September 2001, A'-1, A'-2, B'-1, B'-2, C'-1, C'-2, in December 2001, and D-1, D-2 in March 2002. Flow discharges, vertical velocity profiles and tide were also recorded. The tide gage (in the September 2001 survey only) was located in waters (Grand Lagoon) close to the entrance channel. The discharge and velocity data was measured with a vessel-mounted Acoustic Doppler Current Profiler, or ADCP (Workhorse 1200 kHz, RD Instruments, San Diego, CA), and the tide with an ultrasonic recorder (Model #220, Infinities USA, Daytona Beach, FL). The coordinates of the cross-section end-points are given in Table 4.1.

Table 4.1 Locations of St. Andrew Bay channel cross-sections

Section	Side	Latitude	Longitude	Northing	Easting	Date
A	A-1	30 07.70	-85 43.36	412452.62	1613441.90	09/18/01
A	A-2	30.07.44	-85 43.28	410875.80	1613857.60	09/18/01
B	B-1	30 07.35	-85 43.91	410315.83	1610524.00	09/18/01
B	B-2	30 07.17	-85 43.71	409240.00	1611584.60	09/18/01
A’	A’-1	30 07.18	-85 43.72	409256.63	1611563.75	12/18/01
A’	A’-2	30 07.40	-85 43.91	410626.10	1610534.09	12/18/01
B’	B’-1	30 07.43	-85 43.30	410766.60	1613757.91	12/18/01
B’	B’-2	30 07.68	-85 43.44	412309.71	1613034.11	12/18/01
C’	C’-1	30 07.06	-85 43.90	408542.02	1610606.43	12/18/01
C’	C’-2	30 07.27	-85 44.01	409822.96	1610030.59	12/18/01
D	D-1	30 07.42	-85 43 .32	410714.20	1613635.15	03/28/02
D	D-2	30 07.65	-85 43. 58	412134.85	1612294.58	03/28/02

Measurements were also taken at the new East Pass after it’s reopening in December 2001. The locations of the East Pass cross-section coordinate end points are given in Table 4.2. Flow cross-section and vertical velocity profiles were measured along cross-section E in December 2001 and F in March 2002.

Table 4.2 Locations of East Pass channel cross-sections

Section	Side	Latitude	Longitude	Northing	Easting	Date
E	E-1	30 03.78	-85 37.07	388325.56	1646376.03	12/19/01
E	E-2	30 03.79	-85 37.12	388371.27	1646103.36	12/19/01
F	F-1	30 03.78	-85 37 07	388325.55	1646376.03	03/27/02
F	F-2	30 03 79	-85 37 12	388371.26	1646103.35	03/27/02

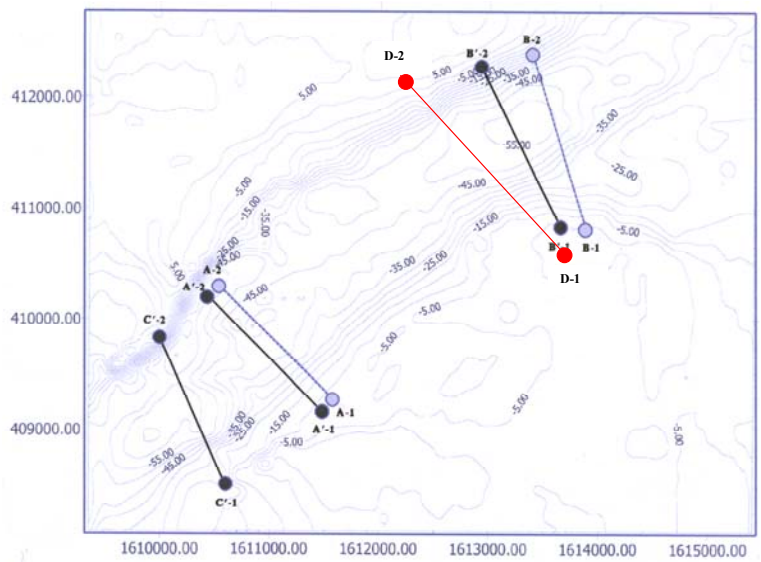

Figure 4.4 St. Andrew Bay Entrance bathymetry and current measurement cross-sections. Depths are in feet below MLLW (source: Jain et al. 2002)

4.2.1 Bathymetry

The bathymetry of the study area is shown in Figure 4.1. During the hydrographic surveys the bottom depth was measured by the ADCP at all cross-sections shown in Figure 4.4. These have been compared with a bathymetric survey of 2000. Figures. 4.5 and 4.6 are example of measurements along cross-sections A and F, respectively. The trends in the two sets of depths are qualitatively (although not entirely) comparable. Areas, mean depths and widths are summarized in Table 4.3.

Table 4.3 Cross-section area, mean depths and width

Section	Cross-section Area (m^2)	Width (m)	Mean Depth (m)
A	6250	493	11.0
B	6600	457	10.6
A’	5210	525	10.0
B’	5640	544	11.0
C’	5220	425	11.5
D	5970	528	11.9
E	255	109	3.0
F	300	85	2.5

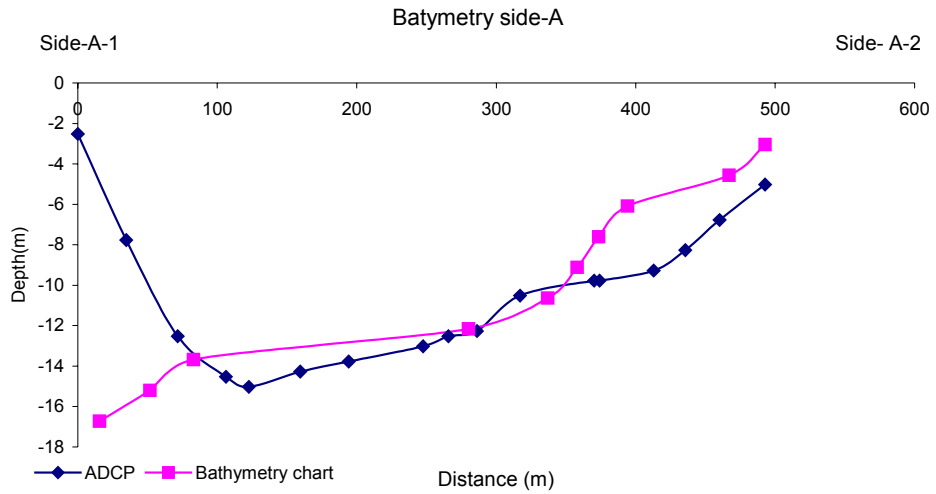

Figure 4.5 Cross-section A in St. Andrew Bay Entrance measured and compared with 2000 bathymetry. Distance is measured from point A-1. The datum is mean tide level (source: Jain and Mehta, 2001)

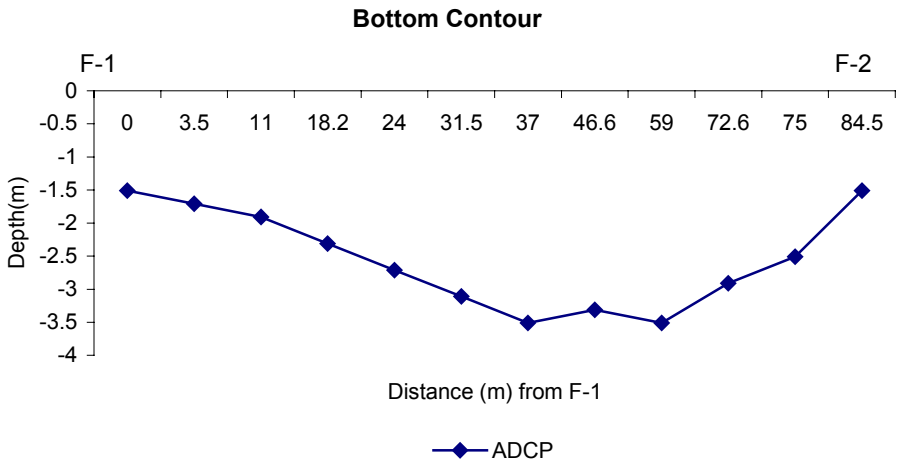

Figure 4.6 Cross-section F in East Pass measured by ADCP. Distance is measured from point F-1. The datum is mean tide level (source: Jain and Mehta, 2002)

4.2.2 Tides

As noted, tide was measured in September 2001 in Grand Lagoon close to the entrance channel, at Lat: 30 07.9667, Long: -85 43.6667. Tide variation in the channel was compared with the predicted National Ocean Service (NOS) tide at St. Andrew Bay channel with reference station at Pensacola after applying the correction factors for the range and the lag. The measured tide is shown in Figure 4.7 and the corresponding NOS tide in Figure 4.8. Both show general similarities, although the measured one should be deemed more accurate. The data indicate a weak semi-diurnal signature with a range variation of 0.11 to 0.18 m. In the month of December and March no tides were measured, only the NOS tides were reported using the tide at Pensacola; see Figure 4.9 and Figure 4.10.

For East Pass the same tide was assumed as for St. Andrew Bay Entrance. Five other NOS stations are also located in the study area as shown in Figure 4.1. The ranges of tides for September 2001, December 2001 and March 2002 at these stations are given in the Table 4.4. These tides were found by applying correction factors for the range and for the lag (see Appendix C). The Gulf tidal range, $2a_o$, was obtained by applying an amplitude correction factor to the tide measured at the Grand Lagoon gauge (see calculations in Appendix C). Semi-diurnal tides were reported in September 2001 with the tidal period of 12.42 h. The tides in December 2001 were of mixed nature with a period of approximately 18 h. In contrast, diurnal tides were reported in March 2002 with the period of 25.82 h. The approximate tide level in each bay was then found by weighted-averaging the tide over the number of stations in that bay. The phase lag between the tides of all the stations were calculated by plotting all the tides in Figure 4.10, and the results are summarized in Table 4.5.

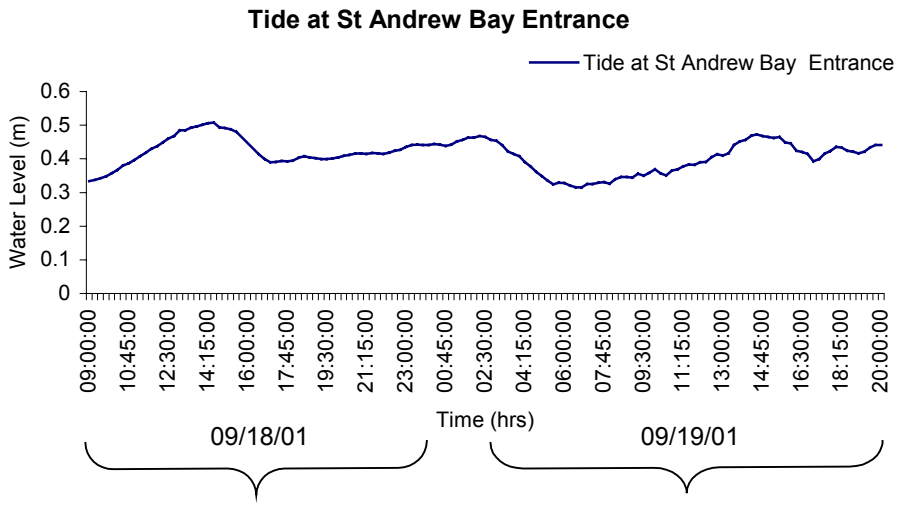

Figure 4.7 Measured tide in Grand Lagoon on September18-19, 2001. The datum is MLLW (source: Jain and Mehta, 2001)

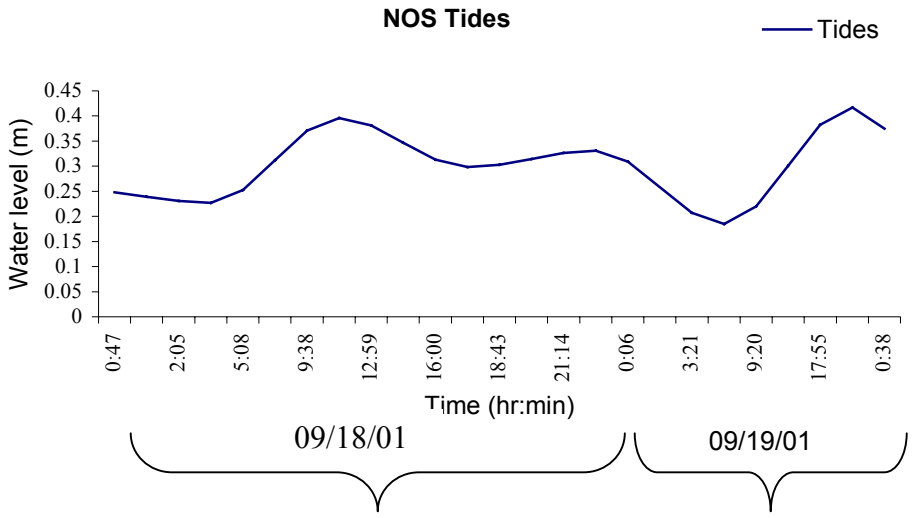

Figure 4.8 NOS predicted tide at St. Andrew Bay Entrance on September18-19, 2001; reference station is Pensacola. The datum is MLLW.

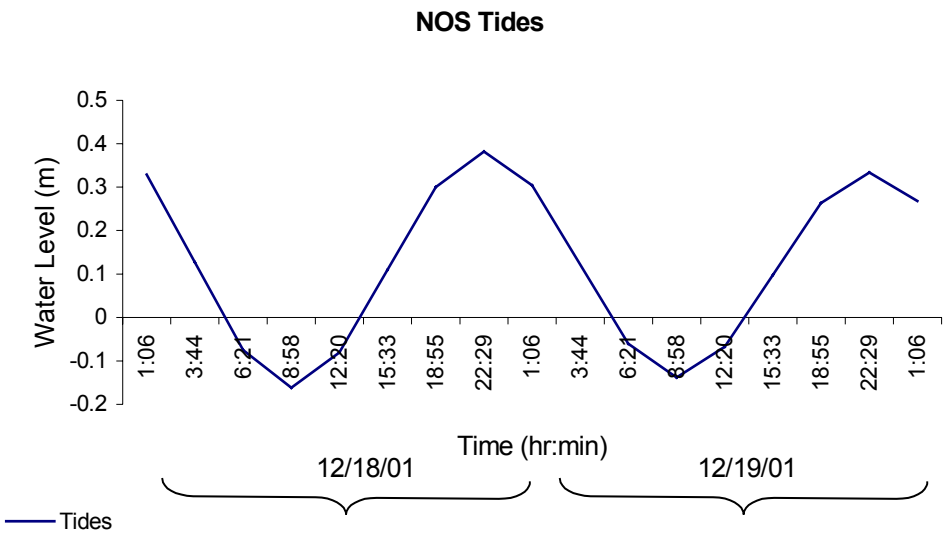

Figure 4.9 NOS predicted tide in St. Andrew Bay Entrance on December 18-19, 2001; reference station is Pensacola. The datum is MLLW.

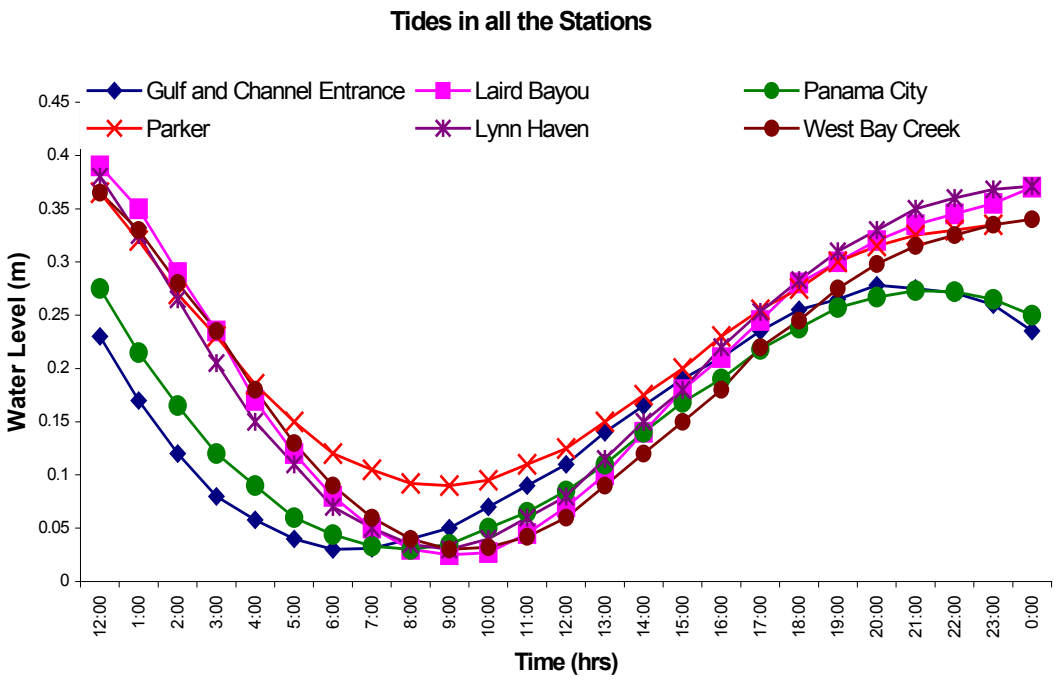

Figure 4.10 Tide at all selected NOS stations in March 2002.

Table 4.4 Tidal ranges in September 2001, December 2001 and March 2002.

S No	Station Name	September Range (m)	December Range (m)	March Range (m)
1	Gulf of Mexico ("Ocean" tide)	0.216	0.572	0.425
2	Laird Bayou, East Bay	0.236	0.624	0.465
3	Parker, East Bay	0.236	0.624	0.465
4	Lynn Haven North Bay	0.236	0.624	0.465
5	Panama City, St. Andrew Bay	0.203	0.535	0.397
6	Channel Entrance, St. Andrew Bay	0.197	0.520	0.386
7	West Bay Creek	0.236	0.624	0.465

Table 4.5 Phase lags between the stations and the ocean tide.

S No	Stations	Time Lag
1	Gulf of Mexico ("Ocean" tide)	0 h
2	Laird Bayou, East Bay	+ 2 h
3	Parker, East Bay	+2 h
4	Lynn Haven North Bay	+2 h
5	Panama City, St. Andrew Bay	+1 h
6	Channel Entrance, St. Andrew Bay	+1 min
7	West Bay Creek	+ 3h

4.2.3 Current and Discharge

Currents and discharges were measured with the ADCP at all the six cross-sections in St. Andrew Bay Entrance (Figure 4.4) and at two cross-sections in East Pass (Figure.4.3). The detailed velocity and discharge curves are shown in Jain and Mehta (2001), Jain et al. (2002) and Jain and Mehta (2002). The measurements are summarized in the Table 4.6.

From Table 4.6 it is observed that the average peak velocity in St. Andrew Bay channel was approximately 0.63 m/s (at or close to the throat section) and at East Pass it was approximately 0.50 m/s. The peak discharge value at St. Andrew was 4200 m^3/s and at East Pass it was 139 m^3/s.

Table 4.6 Characteristic peak velocity and discharge values

Quantity	Velocity (m/s)		Discharge (m^3/s)	
Cross-section	Peak Flood	Peak Ebb	Peak Flood	Peak Ebb
A	0.63	-0.62	4200	3620
B	0.45	-0.34	2980	2250
A’	0.68	-0.69	3620	3920
B’	0.69	-0.66	4061	3876
C’	0.67	-0.77	3480	3750
D	0.42	-0.49	2509	2777
E	0.51	-0.49	139	165
F	0.43	-0.38	114	101

4.3 Tidal Prism

Tidal prism is the volume of water that enters the bay during flood flow. Tidal prism for St. Andrew Bay system was calculated using the approximate formula

$$P = \frac{Q_m T}{\pi C_K} \tag{4.1}$$

where Q_m is the peak discharge (Table 4.6), T is the tidal period (12.42 hrs for September 2001, 18 hrs for December 2001 and 25.82 hrs for March 2002) and the coefficient C_K = 0.86 (Keulegan, 1967). This tidal prism was compared with the O’Brien (1969) relationship of Eq. (4.2), where A_c is the throat area, P the tidal prism on the spring range for sandy inlets in equilibrium, and a and b are the constants:

$$A_c = a\, P^b \tag{4.2}$$

For inlets with two jetties, $a = 7.49\text{x}10^{-4}$ and $b = 0.86$ (Jarrett, 1976). And for inlets without jetty (East Pass), $a = 3.83\text{x}10^{-5}$ and $b = 1.03$. The values of the tidal prism are summarized in Table 4.7. Spring ranges are reported in Table 4.4.

It should be noted that the prism values from the O’Brien relationship are mere estimates.

Table 4.7 Flood and ebb tidal prisms

Quantity	Prism (m^3) from peak discharge		Prism (m^3) from O'Brien	
Cross-sections	Flood	Ebb	Peak Flood	Peak Ebb
A	$7.0x10^7$	$6.0x10^7$	$11.4x10^7$	$10.3x10^7$
A'	$8.6x10^7$	$9.4x10^7$	$09.0x10^7$	$10.4x10^7$
D	$8.6x10^7$	$9.4x10^7$	$10.0x10^7$	$09.7x10^7$
E	$3.3x10^6$	$3.9x10^6$	$03.8x10^6$	$04.6x10^6$
F	$3.9x10^6$	$3.5x10^6$	$03.6x10^6$	$03.6x10^6$

.

CHAPTER 5
RESULTS AND DISCUSSION

5.1 Introduction

There are two aspects of this chapter, one dealing with the hydraulics of the St. Andrew Bay system and the other with its stability. The linearized approach developed in Chapter 2 is used to examine the hydraulics of St. Andrew Bay under different conditions. The model is run as one-inlet/one-bay system for both September 2001 and March 2002. It is also run as a three-inlets/three-bays system in September 2001 when East Pass was closed, and as a three-bays/four-inlets system when East Pass was open in March 2002. Hydraulic parameters related to tides and currents thus obtained are then compared with values from the hydrographic surveys done in September 2001 and March 2002.

In contrast to hydraulics, the (linearized lumped paramter model) inlet stability model developed in Chapter 3 is applied only to St. Andrew Bay. A qualitative approach is developed to discuss the results and graphs have been plotted to show stability variation.

5.2 Hydraulics of St. Andrew Bay

The solution of equations for the linear model, derived in Chapter 2, forms the basis of calculation of the hydraulic parameters characterizing the system. One begins with the basic model of one-inlet (St. Andrew Bay Entrance) and one-bay (St. Andrew Bay) system, when East Pass was closed. As noted the model is then extended to the complete system of three bays (St. Andrew Bay, East Bay and North + West Bays) and

three inlets when East Pass was closed in September 2001, and finally as three bays and four inlets when East Pass was open in March 2002.

5.2.1 Solution of Equations

The solutions of the relevant hydraulic equations are given in Chapter 2. A Matlab program (see Appendix A) was developed to solve the one-inlet bay system as well as the multiple-inlet bay system. The input and output parameters for each system are listed in the tabular form.

5.2.1.1 One-inlet one-bay system

The one-inlet one-bay system is based on solving Eq. (5.1):

$$\hat{\eta}_o - \hat{\eta}_B = \frac{\sigma}{C}\left[\frac{d\hat{\eta}_B}{d\theta}\right] \tag{5.1}$$

The required input and output parameters for this case are given in Table 5.1.

Table 5.1 List of input and output parameters for one-inlet one-bay model.

Input Parameters	
a_o	Ocean tide amplitude (Gulf of Mexico)
T	Time period of tide
a_{B1}	Bay 1 tide amplitude (St. Andrew Bay)
A_{B1}	Bay 1 surface area
L_1	Length of inlet 1 (St. Andrew Bay Entrance)
R_1	Hydraulic radius of inlet 1
A_{c1}	Inlet 1 cross-section area
k	Entrance and exit losses
f	Friction factor
$(\eta_o - \eta_{B1})_{max}$	Maximum ocean-bay tide difference
Output Parameters	
η_{B1}	Bay 1 tide
a_{B1}	Bay 1 tide amplitude
ε_{B1}	Phase difference between bay 1 and ocean tides
u_{max1}	Maximum velocity through Inlet 1
ε_{v1}	Phase difference between velocity in Inlet1 and ocean tide
$(\eta_o - \eta_{B1})_{max}$	Maximum ocean-bay tide difference

5.2.1.2 Three inlets and three bays with one inlet connected to ocean

This system is based on solving Eq. (5.2), Eq. (5.3) and Eq. (5.4):

$$\hat{\eta}_o - \hat{\eta}_{B1} = \frac{\sigma}{C_1}\left[\frac{d\hat{\eta}_{B1}}{d\theta} + \frac{A_{B2}}{A_{B1}}\frac{d\hat{\eta}_{B2}}{d\theta} + \frac{A_{B3}}{A_{B1}}\frac{d\hat{\eta}_{B3}}{d\theta}\right] \tag{5.2}$$

$$\hat{\eta}_{B1} - \hat{\eta}_{B2} = \frac{\sigma}{C_2}\left[\frac{d\hat{\eta}_{B2}}{d\theta}\right] \tag{5.3}$$

$$\hat{\eta}_{B1} - \hat{\eta}_{B3} = \frac{\sigma}{C_4}\left[\frac{d\hat{\eta}_{B3}}{d\theta}\right] \tag{5.4}$$

The required input and output parameters for this case are given in Table 5.2

Table 5.2 List of input and output parameters for the three inlets and three bays model.

Input Parameters	
a_o	Ocean Tide amplitude (Gulf of Mexico)
T	Time period of the tide
a_{B1}	Bay 1 tide amplitude (St. Andrew Bay)
a_{B2}	Bay 2 tide amplitude (East Bay)
a_{B3}	Bay 3 tide amplitude (West Bay)
A_{B1}	Bay 1 surface area
A_{B2}	Bay 2 surface area
A_{B3}	Bay 3 surface area
L_1	Length of inlet 1 (St. Andrew Bay Entrance)
R_1	Hydraulic radius of inlet 1
A_{c1}	Inlet 1 cross-section area
L_2	Length of inlet 2 (connecting East Bay and St. Andrew Bay)
R_2	Hydraulic radius of inlet 2
A_{c2}	Inlet 2 cross-section area
L_4	Length of inlet 4 (connecting West Bay and St. Andrew Bay)
R_4	Hydraulic radius of inlet 4
A_{c4}	Inlet 4 cross-section area
k	Entrance and exit losses
f	Friction factor
$(\eta_o - \eta_{B1})_{max}$	Maximum ocean-bay tide difference
$(\eta_{B1} - \eta_{B2})_{max}$	Maximum Bay 1 and Bay 2 tide difference
$(\eta_{B1} - \eta_{B3})_{max}$	Maximum Bay 1 and Bay 3 tide difference

Table 5.2 (continued)

Output Parameters	
η_{B1}	Bay 1 tide
a_{B1}	Bay 1 tide amplitude
ε_{B1}	Phase lag between bay 1 and ocean tide
η_{B2}	Bay 2 tide
a_{B2}	Bay 2 tide amplitude
ε_{B2}	Phase lag between bay 2 and ocean tide
η_{B3}	Bay 3 tide
a_{B3}	Bay 3 tide amplitude
ε_{B3}	Phase lag between bay 3 and ocean tide
u_{max1}	Maximum velocity through Inlet 1
ε_{v1}	Phase difference between velocity of Inlet 1 and the ocean tide
u_{max2}	Maximum velocity through Inlet 2
ε_{v2}	Phase difference between velocity of Inlet 2 and the ocean tide
u_{max4}	Maximum velocity through inlet 4
ε_{v4}	Phase difference between velocity of Inlet 4 and the ocean tide
$(\eta_o - \eta_{B1})_{max}$	Maximum ocean-bay tide difference
$(\eta_{B1} - \eta_{B2})_{max}$	Maximum Bay 1 and Bay 2 tide difference
$(\eta_{B1} - \eta_{B3})_{max}$	Maximum Bay 1 and Bay 3 tide difference

5.2.1.3 Three inlets and three bays with two inlets connected to ocean

This system is based on solving Eq. (5.5), Eq. (5.6) and Eq. (5.7):

$$\hat{\eta}_o - \hat{\eta}_{B1} = \frac{\sigma}{C_1 + C_3}\left[\frac{d\hat{\eta}_{B1}}{d\theta} + \frac{A_{B2}}{A_{B1}}\frac{d\hat{\eta}_{B2}}{d\theta} + \frac{A_{B3}}{A_{B1}}\frac{d\hat{\eta}_{B3}}{d\theta}\right] \tag{5.5}$$

$$\hat{\eta}_{B1} - \hat{\eta}_{B2} = \frac{\sigma}{C_2}\left[\frac{d\hat{\eta}_{B2}}{d\theta}\right] \tag{5.6}$$

$$\hat{\eta}_{B1} - \hat{\eta}_{B3} = \frac{\sigma}{C_4}\left[\frac{d\hat{\eta}_{B3}}{d\theta}\right] \tag{5.7}$$

The required input and output parameters for this case are given in Table 5.3.

Table 5.3 List of Input and Output Parameters for the four inlets and three bays model.

Input Parameters	
a_o	Ocean Tide Amplitude (Gulf of Mexico)
T	Time period of the tide
a_{B1}	Bay 1 tide amplitude (St. Andrew Bay)
a_{B2}	Bay 2 tide amplitude (East Bay)
a_{B3}	Bay 3 tide amplitude (West Bay)
A_{B1}	Bay 1 surface area
A_{B2}	Bay 2 surface area
A_{B3}	Bay 3 surface area
L_1	Length of inlet 1 (St. Andrew Bay Entrance)
R_1	Radius of inlet 1
A_{c1}	Inlet 1 cross-section area
L_2	Length of inlet 2 (connecting East Bay and St. Andrew Bay)
R_2	Radius of inlet 2
A_{c2}	Inlet 2 cross-section area
L_3	Length of inlet 3 (East Pass)
R_3	Radius of inlet 3
A_{c3}	Inlet 3 cross-section area
L_4	Length of inlet 4 (connecting West Bay and St. Andrew Bay)
R_4	Radius of inlet 4
A_{c4}	Inlet 4 cross-section area
k	Entrance and exit losses
f	Friction factor
$(\eta_o - \eta_{B1})_{max}$	Maximum ocean-bay tide difference
$(\eta_{B1} - \eta_{B2})_{max}$	Maximum Bay 1 and Bay 2 tide difference
$(\eta_{B1} - \eta_{B3})_{max}$	Maximum Bay 1 and Bay 3 tide difference
Output Parameters	
η_{B1}	Bay 1 tide
a_{B1}	Bay 1 tide amplitude
ε_{B1}	Phase lag between bay 1 and ocean tide
η_{B2}	Bay 2 tide
a_{B2}	Bay 2 tide amplitude
ε_{B2}	Phase lag between bay 2 and ocean tide
η_{B3}	Bay 3 tide
a_{B3}	Bay3 tide amplitude
ε_{B3}	Phase lag between bay 3 and ocean tide
u_{max1}	Maximum velocity through Inlet 1
ε_{v1}	Phase difference between velocity of Inlet 1 and the ocean tide
u_{max2}	Maximum velocity through Inlet 2

Table 5.3 Continued)

Output Parameters	
ε_{v2}	Phase difference between velocity of Inlet 2 and the ocean tide
u_{max3}	Maximum velocity through Inlet 3
ε_{v3}	Phase difference between velocity of Inlet 3 and the ocean tide
u_{max4}	Maximum velocity through Inlet 4
ε_{v4}	Phase difference between velocity of Inlet 4 and the ocean tide
$(\eta_o - \eta_{B1})_{max}$	Maximum ocean-bay tide difference
$(\eta_{B1} - \eta_{B2})_{max}$	Maximum Bay 1 and Bay 2 tide difference
$(\eta_{B1} - \eta_{B3})_{max}$	Maximum Bay 1 and Bay 3 tide difference

5.2.2 Input Parameters

Table 5.4 provides the input values for all the three cases of the model as described in Section 5.2.

1 The amplitude in each bay is found by applying a weighting factor proportional to the tide station contribution to the total bay area.

2 Initial values are assumed for $(\eta_o - \eta_{B1})_{max}$, $(\eta_{B1} - \eta_{B2})_{max}$ $(\eta_{B1} - \eta_{B3})_{max}$ for the initial calculation. The September 2001 tide showed a semidiurnal signal, with a period of 12.42 h. The tide in March 2002 showed diurnal signature with a period of 25.82 h. The model was run three times for three different cases as described in Section 5.2. Details regarding all input parameters are found in Jain and Mehta (2002), and are also summarized in Chapter 4. Table 5.4 gives values of all input parameters required for the model.

Table 5.4 Input parameters for the hydraulic model.

Input Parameters	Values		Remarks
	Sept 2001	March 2002	
a_o	0.109 m	0.212 m	Calculated from UF tide gauge data, calculations shown in Appendix C.
T	12.42 h	25.82 h	NOS Tides Tables.
a_{B1}	0.103 m	0.201 m	Calculated in proportion to the contributing tide at station.
a_{B2}	0.115 m	0.226 m	
a_{B3}	0.118 m	0.233 m	
A_{B1}	74 km^2		From the USGS topographic maps.
A_{B2}	54 km^2		
A_{B3}	155 km^2		

Table 5.4 (continued)

Input Parameters	Values		Remarks
	Sept 2001	March 2002	
L_1	1340 m		Measured in survey
R_1	10 m		
A_{c1}	6300 m^2		
L_2	1000 m		From the USGS topographic maps. A_{c2}, A_{c3}, A_{c4} are zero for one inlet bay case
R_2	9 m		
A_{c2}	1.9×10^4 m^2		
L_4	1000 m		
R_4	12 m		
A_{c4}	9.7×10^3 m^2		
L_3	400 m		Measured in survey. A_{c3} is zero for three-bays and three-inlets case.
R_3	3 m		
A_{c3}	255 m^2		
k	1.05		
f	0.025		
$(\eta_o - \eta_{B1})_{max}$	0.037	0.036	Assumed initial values. Calculations are shown in appendix C
$(\eta_{B1} - \eta_{B2})_{max}$	0.060	0.063	
$(\eta_{B1} - \eta_{B3})_{max}$	0.099	0.998	

5.2.3 Model Results and Comparison with Data

Model results are given in Table 5.5.

Table 5.5 Model results and measurements.

One Inlet One Bay System, September 2001			
Output parameters	Model	Measurement	%error
a_{B1}	0.10 m	0.10 m	0%
ε_{B1}	0.36 rad	0.34 rad	6%
$u_{c1\,max}$	0.65 m/s	0.63 m/s	3%
ε_{v1}	-1.20 rad	-1.22 rad	2%
$(\eta_o - \eta_{B1})_{max}$	0.038	0.036	6%
Three Bay - Three Inlets System, September 2001			
a_{B1}	0.10 m	0.10 m	0%
ε_{B1}	0.34 rad	0.34 rad	0%
a_{B2}	0.10 m	0.11 m	9%
ε_{B2}	0.37 rad	0.91 rad	59%
a_{B3}	0.10 m	0.12 m	17%
ε_{B3}	0.54 rad	1.26 rad	57%

Table 5.5 (continued)

Three Bay - Three Inlets System, September 2001			
Output parameters	Model	Measurement	%error
$u_{c1\ max}$	0.62 m/s	0.63 m/s	2%
ε_{v1}	-1.11 rad	-1.20 rad	7%
$u_{c2\ max}$	0.04 m/s	Not measured	-
ε_{v2}	-1.21 rad	Not measured	-
$u_{c4\ max}$	0.20 m/s	Not measured	-
ε_{v4}	-1.04 rad	Not measured	-
$(\eta_o - \eta_{B1})_{max}$	0.037	0.037	0%
$(\eta_{B1} - \eta_{B2})_{max}$	0.003	0.060	95%
$(\eta_{B1} - \eta_{B3})_{max}$	0.020	0.098	80%
One Inlet One Bay System, March 2002			
a_{B1}	0.20 m	0.20 m	0%
ε_{B1}	0.17 rad	0.17 rad	0%
$u_{c1\ max}$	0.63 m/s	0.65 m/s	3%
ε_{v1}	-1.40 rad	-1.40 rad	0%
$(\eta_o - \eta_{B1})_{max}$	0.036	0.036	0%
Three Bay – Four Inlets System, March 2002			
a_{B1}	0.21 m	0.20 m	5%
ε_{B1}	0.16 rad	0.16 rad	0%
a_{B2}	0.21 m	0.22 m	5%
ε_{B2}	0.18 rad	0.44 rad	59%
a_{B3}	0.21 m	0.23 m	9%
ε_{B3}	0.26 rad	0.60 rad	57%
$u_{c1\ max}$	0.60 m/s	0.65 m/s	8%
ε_{v1}	-1.35 rad	-1.40 rad	4%
$u_{c2\ max}$	0.04 m/s	Not measured	-
ε_{v2}	-1.40 rad	Not measured	-
$u_{c3\ max}$	0.60 m/s	0.55 m/s	9%
ε_{v3}	-1.35 rad	-1.40 rad	4%
$u_{c4\ max}$	0.22 m/s	Not measured	-
ε_{v4}	-1.31 rad	Not measured	-
$(\eta_o - \eta_{B1})_{max}$	0.035	0.035	0%
$(\eta_{B1} - \eta_{B2})_{max}$	0.003	0.063	95%
$(\eta_{B1} - \eta_{B3})_{max}$	0.012	0.010	20%

It is evident from Table 5.5 that the linear model gives good results. The percent error decreases if the system is modeled as a three-bay system, which is actually the case. Velocity and tide amplitudes are within reasonably small error limits. The phase differences between ocean (Gulf) and bay tides from data are very approximate as they

are calculated based on weighted-average tides at selected stations. Moreover, there are very few stations to yield a good value of tide for a bay. Note that the input values for $(\eta_o - \eta_{B1})_{max}$, $(\eta_{B1} - \eta_{B2})_{max}$ $(\eta_{B1} - \eta_{B3})_{max}$ is also approximate. Sample calculation for $(\eta_o - \eta_{B1})_{max}$, $(\eta_{B1} - \eta_{B2})_{max}$ $(\eta_{B1} - \eta_{B3})_{max}$ is given in Appendix C.

5.3 Stability Analysis

The stability analysis developed in Chapter 3 is now applied to St. Andrew Bay system. This analysis is done for a two-inlet bay system using van de Kreeke's (1990) linearized lumped parameter model. The two inlets, to which the model is applied, are St. Andrew Bay Entrance and the new East Pass opened in December 2002. Calculations related to stability are given in Appendix D. A Matlab program (Appendix D) has also been developed for doing the analysis and generating equilibrium flow curves for the two inlets. There are two programs, one for rectangular channel cross-section and another for triangular channel cross-sections.

5.3.1 Input Parameters

Input parameters required for the Matlab program (Appendix D) are listed in Table 5.6. Since the objective was to study the effect of bay area on the stability because the results are sensitive to it, it is held constant for a particular set of calculation, but is varied for generating different sets of equilibrium flow curves. Similarly the length of East Pass, believed to have an uncertain value due to the complex bay shoreline and bathymetry in that region is also varied to study its effect on the system.

Table 5.6 Input parameters for stability analysis.

Input Parameters for December 2001		
a_o	0.26 m	Amplitude of ocean tide
T	18.0 hrs	Time period of tide
A_B	74-105 km^2	Area of bay (St. Andrew Bay) (varied from 74 to 105 km^2)
Inlet 1		
u_{eq1}	0.40 m/s	Equilibrium velocity for Inlet 1 (see Appendix D)
W_1	525 m	Width of Inlet 1
L_1	1340 m	Length of Inlet 1
a_1	0.138	Constant for triangular cross-section for Inlet 1 (see Appendices C and D)
F_1	0.004	Friction coefficient for Inlet 1
Inlet 2		
u_{eq2}	0.45 m/s	Equilibrium velocity for Inlet 2 (see Appendix D)
W_2	300 m	Width of Inlet 2
L_2	500-2000 m	Length of Inlet 2 (East Pass) (varied from 500 m to 2000 m)
a_2	0.187	Constant for triangular cross-section for Inlet 2 (see Appendices C and D)
F_2	0.004	Friction coefficient for Inlet 2

5.3.2 Results and Discussion

As noted, it is found that two inlets can never be unconditionally stable simultaneously in one bay. The bay area has a large effect on the stability of the inlets. Table 5.7 summarizes this effect. It is clear that with a small increase in bay area the inlets become stable. This is also demonstrated with the help of equilibrium flow curve in the Figure 5.1, Figure 5.2 and Figure 5.3 for rectangular cross-section and Figure 5.7 and Figure 5.9 for triangular cross-section. The cross-sectional area pair during December 2001 (Table 4.3) [5210, 255] is shown by the dot. Figure 5.1 and Figure 5.7 have small bay areas, and the dot lies outside the equilibrium flow curve indicating that both inlets are unstable. As the bay area increases St. Andrew becomes stable (Figure 5.2 and Figure 5.7), and a further increase in bay area also stabilizes East Pass (Figure 5.3 and Figure 5.9). However, in reality we cannot increase the bay area beyond a reasonable limit, because then the basic assumption of bay tide fluctuating evenly in the bay does not hold.

Moreover, in a shallow bay the effect of dissipation of tidal energy cannot be ignored, especially if the bay is large. Also as per Figure 3.5 two inlets are not stable simultaneously.

An increase in the length of East Pass has a destabilizing effect on that inlet as shown in the Table 5.7. Note also that for a rectangular cross-section (Figure 5.3) with the length of East Pass of 500m, this inlet is stable, whereas with a length of 2000 m (Figure 5.6) the inlet is instable. This is because as the length increases the dissipation increases. Friction dominated losses, (F = 0.004, R = 3m $\left(2FL/R\right)$) for East Pass with 500 m length is 1.33, where as that for 2000 m length it is 5.33. The same cases occur in Figure 5.9 and Figure 5.12.

The other effects on the stability model are the approximation in the cross-section of the inlet. It is clear that triangular cross-section is a better approximation than rectangular section, because with the same parameters for rectangular cross-section in Figure 5.6, East Pass is predicted to be unstable whereas in Figure 5.12 for triangular cross-section, East Pass is stable even though barely, which is not believed to be the case for this newly opened inlet.

Table 5.8 gives the qualitative indication of the stability. The various zones mentioned in the Table 5.8 are described in Section 3.4 and Figure 3.6. It is clear from these results that St. Andrew is a stable inlet (for a realistic bay area) as opposed to East Pass. This is also evident from the Figure 3.5, which shows that two inlets cannot be stable simultaneously, because we for unconditional stability, need four real points of intersection of equilibrium flow curve and none of the solutions (neither rectangular cross-section nor triangular cross-section) gives four real solution.

The model does not yield an analytic solution for a more realistic parabolic cross-section. Another weakness is due to the assumptions made in Chapter 3 including a bay area in which the tide is spatially always in-phase, and simple a harmonic function for tide. These assumptions are not always satisfied.

Table 5.7 Effect of change in bay area and length of East Pass.

Rectangular cross-section			
Run No.	Bay area (km^2)	East Pass Length (m)	Result
1	74	500	Both inlets unstable (Figure 5.1)
2	90	500	St. Andrew becomes stable (Figure 5.2)
3	105	500	St. Andrew stable, East Pass barely stable (Figure 5.3)*
4	74	2000	Both inlets unstable (Figure 5.4)
5	90	2000	St. Andrew barely stable (Figure 5.5)
6	105	2000	St. Andrew stable, East Pass unstable (Figure 5.6)
Triangular cross-section			
7	74	500	Both inlets unstable Figure (5.7)
8	90	500	St. Andrew becomes stable (Figure 5.8)
9	105	500	Both inlets stable (Figure 5.9)*
10	74	2000	Both inlets unstable (Figure 5.10)
11	90	2000	St. Andrew stable (Figure 5.11)
12	105	2000	St. Andrew stable, East Pass just stable (Figure 5.12)*

* Two inlets cannot be simultaneously stable, because according to Figure 3.5, for unconditional stability we need four real points of intersection of equilibrium flow curve, which is not possible in either rectangular cross-section solution nor triangular cross-section solution.

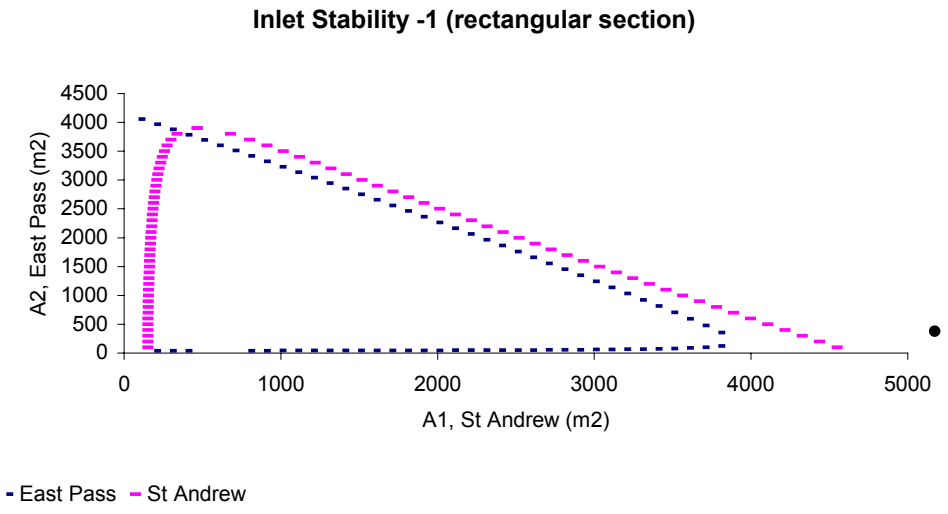

Figure 5.1 Equilibrium flow curves for rectangular cross-sections, Run No. 1.

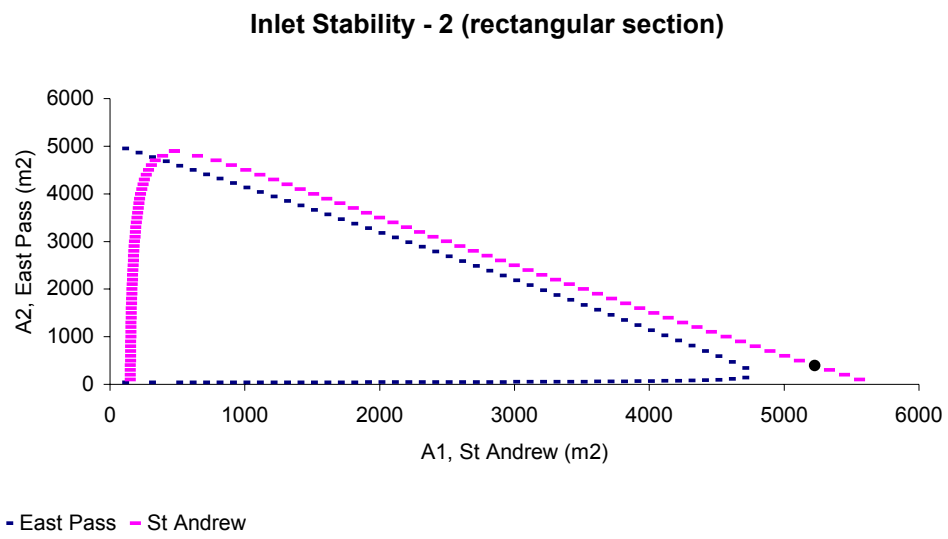

Figure 5.2 Equilibrium flow curves for rectangular cross-sections, Run No. 2.

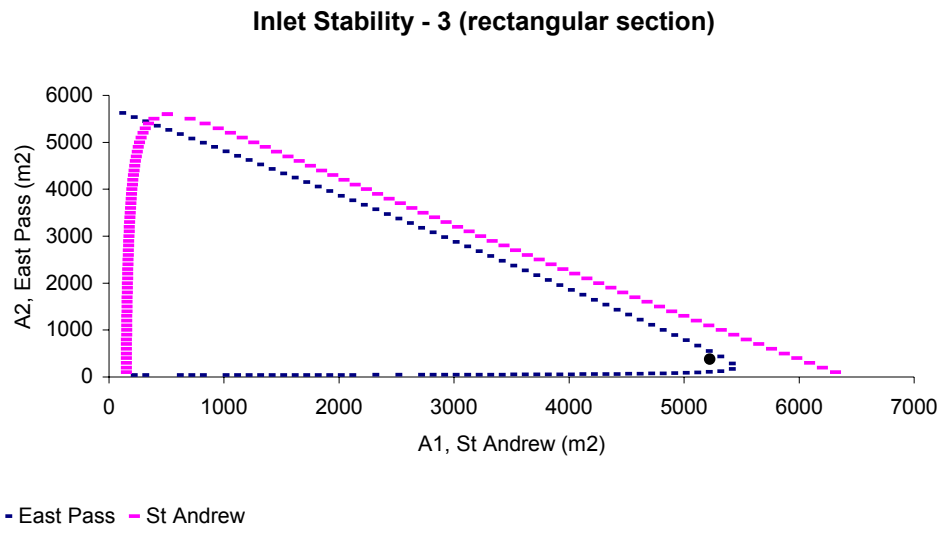

Figure 5.3 Equilibrium flow curves for rectangular cross-sections, Run No. 3.

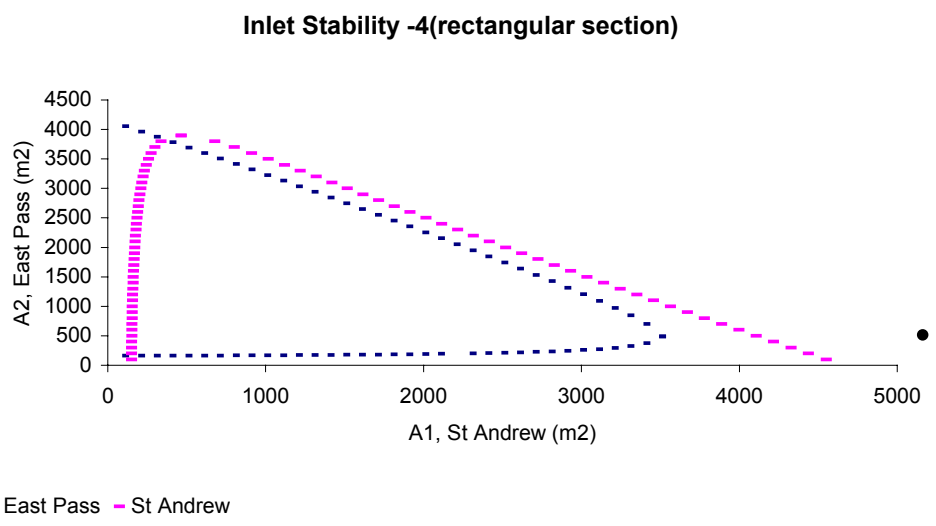

Figure 5.4 Equilibrium flow curves for rectangular cross-sections, Run No. 4.

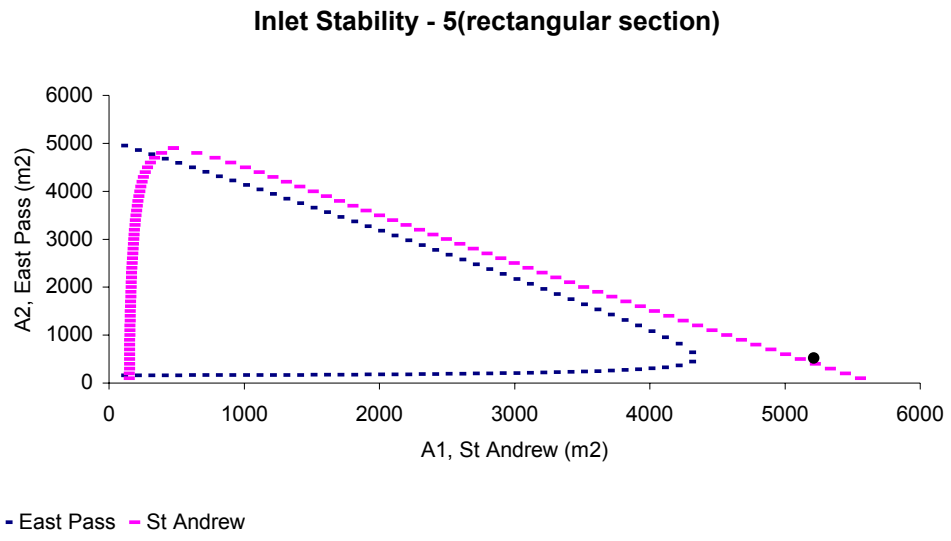

Figure 5.5 Equilibrium flow curves for rectangular cross-sections, Run No. 5.

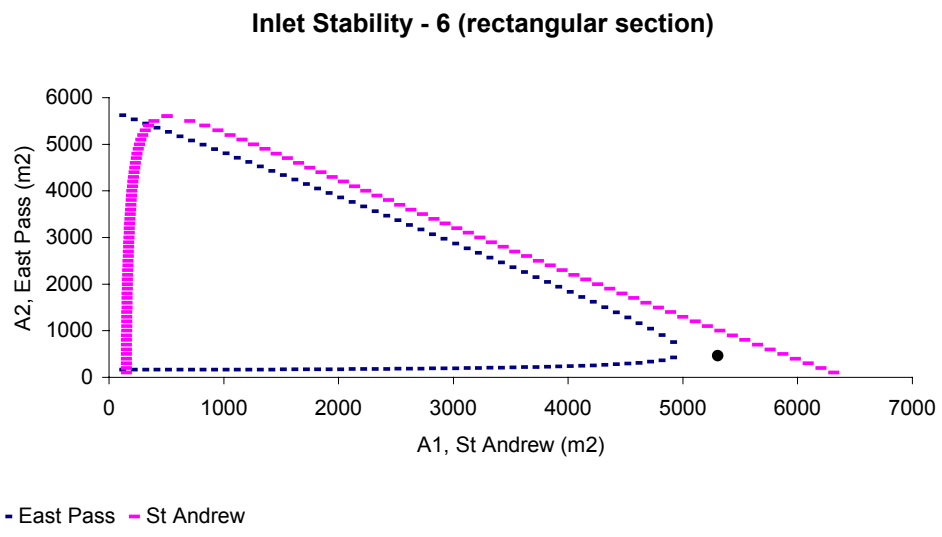

Figure 5.6 Equilibrium flow curves for rectangular cross-sections, Run No. 6.

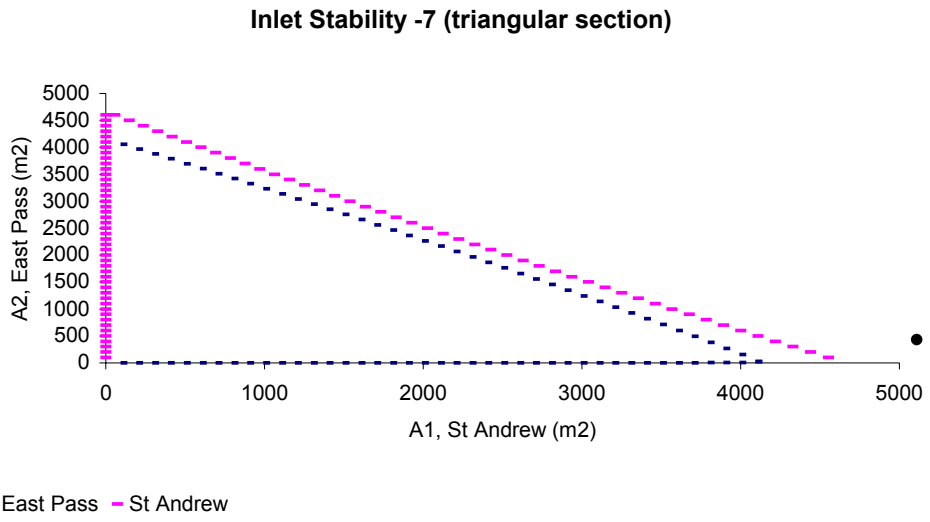

Figure 5.7 Equilibrium flow curves for triangular cross-sections, Run No. 7.

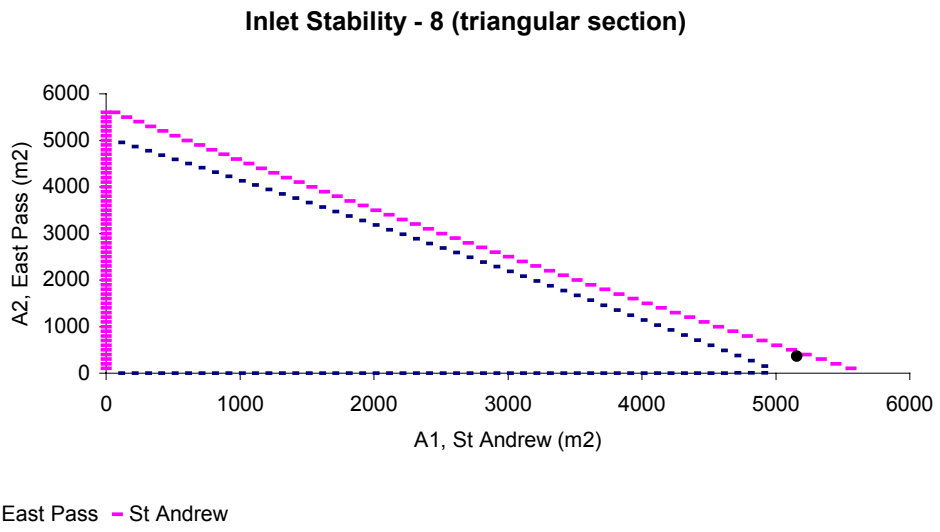

Figure 5.8 Equilibrium flow curves for triangular cross-sections, Run No. 8.

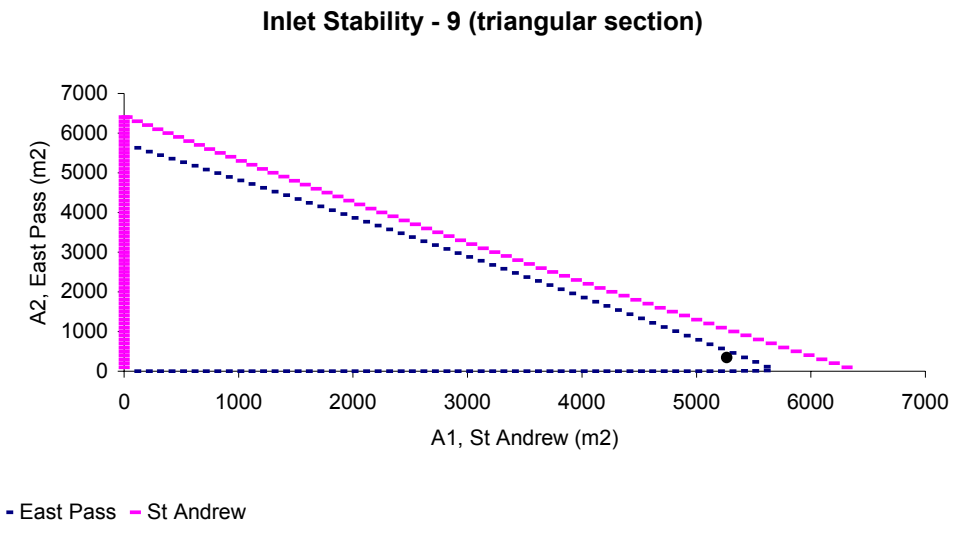

Figure 5.9 Equilibrium flow curves for triangular cross-sections, Run No. 9.

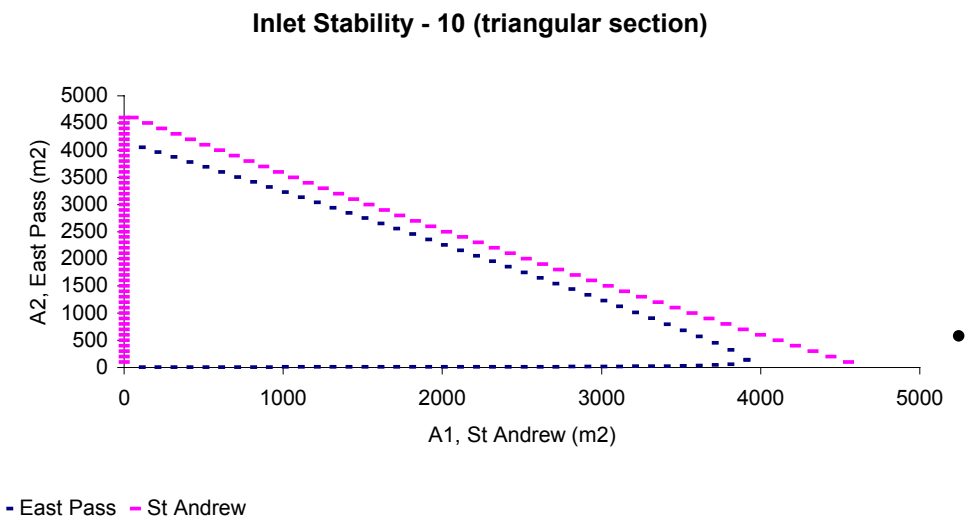

Figure 5.10 Equilibrium flow curves for triangular cross-sections, Run No. 10

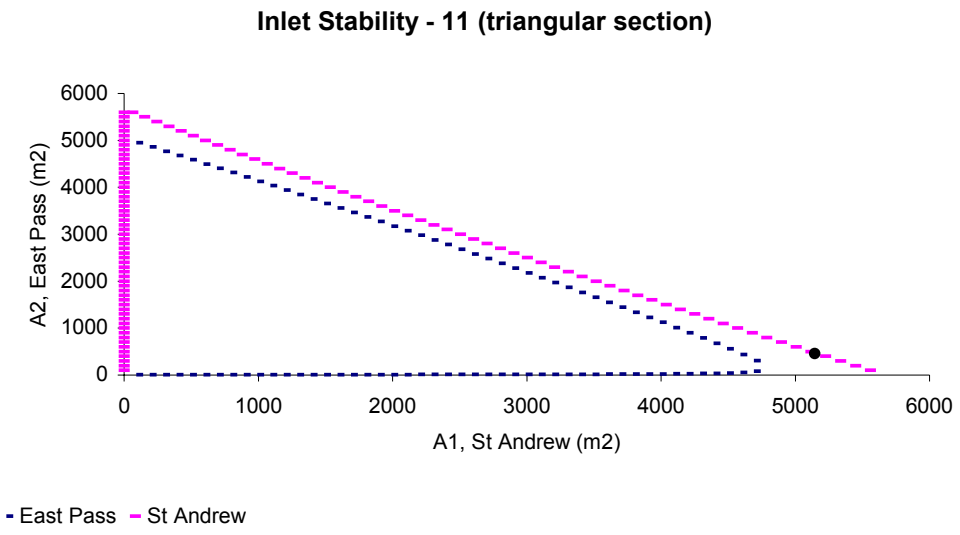

Figure 5.11 Equilibrium flow curves for triangular cross-sections, Run No. 11.

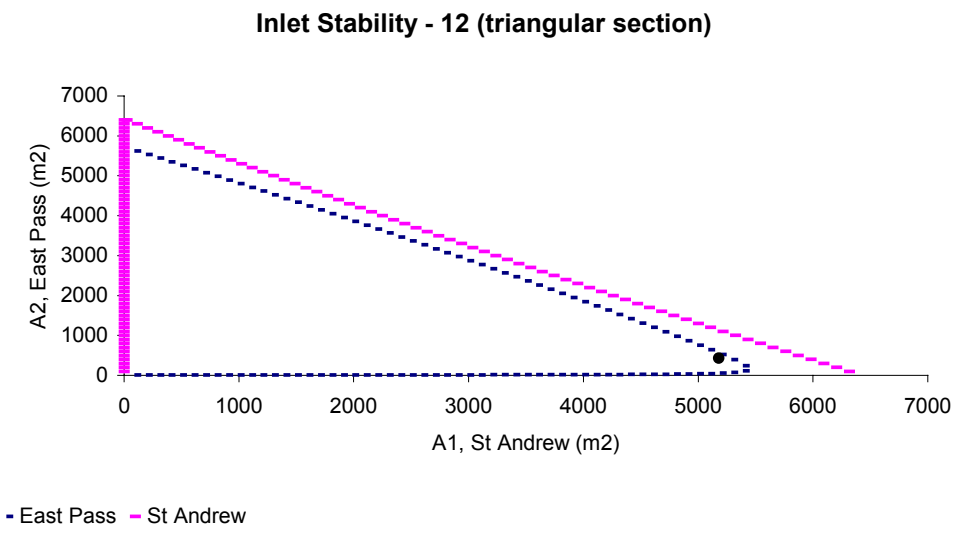

Figure 5.12 Equilibrium flow curves for triangular cross-sections, Run No. 12.

Table 5.8 Stability observations for St. Andrew Bay Entrance and East Pass.

Figure	Placement of cross-sectional area pair [A_1, A_2], (black dot)	Observations
Figure 5.1	Zone-1	Both inlets are unstable
Figure 5.2	Zone-2	St. Andrew Bay Entrance is stable
Figure 5.3	Zone-4	Only one is stable i.e. St. Andrew[a]
Figure 5.4	Zone-1	Both inlets are unstable
Figure 5.5	Zone-2	St. Andrew Bay Entrance is stable
Figure 5.6	Zone-2	St. Andrew Bay Entrance is stable
Figure 5.7	Zone-1	Both inlets are unstable
Figure 5.8	Zone-2	St. Andrew Bay Entrance is stable
Figure 5.9	Zone-4	Only one is stable i.e. St. Andrew[a]
Figure 5.10	Zone-1	Both inlets are unstable
Figure 5.11	Zone-2	St. Andrew Bay Entrance is stable
Figure 5.12	Zone-4	Only one is stable i.e. St. Andrew[a]

[a] As per Figure 3.6, it is clear that even in Zone-4 only one inlet is stable, this is further clarified from Figure 3.5, which shows that only one inlet can be stable at one time.

.

CHAPTER 6
CONCLUSIONS

6.1 Summary

St. Andrew Bay, which is a composite of three interconnected bays (St. Andrew Bay proper, West Bay + North Bay and East Bay) is located in Bay County on the Gulf of Mexico coast of Florida's panhandle. It is part of a three-bay and two-inlet complex. One of these inlets is St. Andrew Bay Entrance and the other is East Pass, which are both connected to St. Andrew Bay on one side and the Gulf on the other. Prior to 1934, East Pass was the natural connection between St. Andrew Bay and the Gulf. In 1934, St. Andrew Bay Entrance (Figure 4.2) was constructed 11 km west of East Pass through the barrier island to provide a direct access between the Gulf and Panama City. The interior shoreline of the entrance has continually eroded since it's opening. East Pass was closed in 1998, which is believed to be due to the opening of the St. Andrew Bay Entrance.

In December 2001, a new East Pass was opened (Figure 4.3), and the effect of this new inlet is presently being monitored over the entire system. Accordingly, the objective of the present work was to examine the hydraulics of the newly formed two-("ocean") inlet/three-bay system and its hydraulic stability, especially as it relates to East Pass.

The first aspect of the tasks performed to meet this objective was the development of equations for the linearized hydraulic model for the system of three bays and four inlets (two ocean and two between bays), and solving and applying them to the St. Andrew Bay system. The second aspect was the development of the ocean inlet stability criteria using the Escoffier (1940) model for one inlet and one bay and extending this

model to the two ocean inlets and a bay. Stability analysis for the St. Andrew Bay system was then carried out using the linearized lumped parameter model of van de Kreeke (1990).

6.2 Conclusions

The following are the main conclusions of this study:

1 If the system is modeled as a three-bay system as compare to a one-bay system, the error in the phase difference, $\varepsilon_{B1,}$ decreases from 6% to 0% and in the velocity amplitude from 3% to 2%. Moreover the error in maximum head difference, $(\eta_o - \eta_{B1})_{max}$, also decreases from 6% to 0%.

2 The amplitudes of velocities and bay tides are within ±5%, which is a reasonably small error band. The percent error for St. Andrew Bay is almost 0%, and for the other bays it is within ±20%.

3 The bay area has a significant effect on the stability of the two inlets. At a bay area of 74 km^2 both inlets are unstable. Increasing it by 22% to 90 km^2 stabilizes St. Andrew Bay Entrance, and by 42% to 105 km^2 stabilizes East Pass as well.

4 Two inlets can never be simultaneously unconditionally stable.

5 Keeping the bay area at 105 km^2 and increasing the length of East Pass from 500 m to 2000 m destabilizes this inlet because as the length increases the dissipation in the channel increases as well.

6 A triangular channel cross-section is a better approximation than a rectangular one, because given the same values of all other hydraulic parameters, St. Andrew Bay Entrance with a rectangular cross-section is found to be barely stable, whereas with a triangular cross-section it is found to be stable, as is the case.

6.3 Recommendations for Further Work

Accurate numerical values required for the stability analysis of a complex inlet-bay system can only be obtained by using a two- (or three)-dimensional tidal model to describe the hydrodynamics of the bay.

Freshwater discharges from the rivers into the bay should be incorporated through numerical modeling.

Including a more realistic assumption for the channel cross-section can improve the stability analysis.

APPENDIX A
ALGORITHMS FOR MULTIPLE INLET-BAY HYDRAULICS

A.1 Introduction

The linearized approach described in Chapter 2 has been used to evaluate the hydraulic parameters of the multiple inlet bay system. The differential equations, developed by this approach (Chapter 2), Eq. (2.100), Eq. (2.101) and Eqs (2.102), are solved in Matlab Program-1 (given below). These are the general equations for four inlets and three bays system. These equations can be used to solve from one bay system to the complex three bays system. Note that for solving Program-1, the Matlab version should have a symbolic toolbox. The present program is solved in Matlab release 6.1. The solution from Program-1 is used as input to Program-2 (given below). The required input parameters and output for Program-2 are listed in Table 5.3 of Chapter 5.

A.2 Program-1

```
%UNIVERSITY OF FLORIDA
%CIVIL AND COASTAL ENGINEERING DEPARTMENT
%PROGRAM FOR SOLVING THE EQS 2.100, 2.101, 2.102
% ALL CONSTANTS DEFINED IN CHAPTER 2

clear all
syms a b c A B
t1=sym('theta1')
t2=sym('theta2')
t3=sym('theta3')
r1=sym('a1*exp(-i*t1)')
r2=sym('a2*exp(-i*t2)')
r3=sym('a3*exp(-i*t3)')
C=[a*i+1 a*A*i a*B*i;-1 b*i+1 0;-1 0 c*i+1]
D=[1;0;0]
%END
```

A.3 Program-2

```
%UNIVERSITY OF FLORIDA
%CIVIL AND COASTAL ENGINEERING DEPARTMENT
%PROGRAM FOR CALCULATION OF MULTIPLE INLET-BAY HYDRUALICS
%FOR ONE -INLET BAY CASE, FOR Ac2, Ac3, Ac4 EQUAL TO ZERO
%INLET 1 AND INLET 3 CONNECTS BAY1 TO THE OCEAN

clear all
g=9.81;
ao=0.212;%ocean tide amplitude
theta=0;%ocean tide phase
etao=ao*cos(theta);%ocean tide
T=25.82;%time period
q=2*pi/(T*3600)%sigma
k=1.05;% entrance and exit loss
f=0.025;%friction factor
aB1=0.201;%approximate amplitude of bays
aB2=0.226;
aB3=0.2325;
%m1=max(eta0-etab1),m2=max(etab1-etab2),m3=max(etab1-etab3)
m1=0.023;
m2=0.0527;
m3=0.123;
%Inlet 1
L1=1340;%Length of inlet
R1=10;%hydraulic radius
Ac1=6300;%CROSS-SECTION AREA of the inlet
F1=k+(f*L1)/(4*R1);%friction factor F includes ken kex fL/4R

%Inlet 2
L2=1000;%Length of inlet
R2=9;%hydraulic radius
Ac2=1.9*10^4;%CROSS-SECTION AREA of the inlet, it is zero for one inlet bay case
F2=k+(f*L2)/(4*R2);%friction factor F includes ken kex fL/4R

%Inlet 3
L3=400;%Length of inlet
R3=3;%hydraulic radius
Ac3=255;%CROSS-SECTION AREA of the inlet
F3=k+(f*L3)/(4*R3);%friction factor F includes ken kex fL/4R

%Inlet 4
L4=1000;%Length of inlet
R4=12;%hydraulic radius
Ac4=9.7*10^3;%CROSS-SECTION AREA of the inlet
F4=k+(f*L4)/(4*R4);%friction factor F includes ken kex fL/4R
```

```
%bay1 area
AB1=74*10^6;
%bay2 area
AB2=54*10^6;
%bay3 area
AB3=155*10^6;

%calculations
CDL1=sqrt(ao/(m1*F1))
CDL2=sqrt(aB1/(m2*F2))
CDL3=sqrt(ao/(m1*F3))
CDL4=sqrt(aB1/(m3*F4))

C1=CDL1*Ac1/AB1*sqrt(2*g/ao)
C2=CDL2*Ac2/AB2*sqrt(2*g/aB1)
C3=CDL3*Ac3/AB1*sqrt(2*g/ao)
C4=CDL4*Ac4/AB3*sqrt(2*g/aB1)

%ALL THE CONSTANTS ARE DEFINED IN THE THESIS
a=q/(C1+C3)
if Ac2==0
  b=0
else   b=q/C2
end

if Ac4==0
  c=0
else
  c=q/C4
end

A=AB2/AB1
B=AB3/AB1
r1=(c-i)*(b-i)/(-i*a*A+i*a*c*b+a*c-i*c-i*b-1+c*b-i*a*B+a*b-
i*a+a*B*b+a*A*c)%SOLUTIONS ARE OBTAINED FROM ANOTHER
r2=-i*(c-i)/(-i*a*A+i*a*c*b+a*c-i*c-i*b-1+c*b-i*a*B+a*b-
i*a+a*B*b+a*A*c)%MATLAB PROGRAM WHICH HAS SYMBOLLIC TOOLBOX.
r3=-i*(b-i)/(-i*a*A+i*a*c*b+a*c-i*c-i*b-1+c*b-i*a*B+a*b-i*a+a*B*b+a*A*c)
aB1=abs(r1)*ao
eB1=-angle(r1)
aB2=abs(r2)*ao
eB2=-angle(r2)
aB3=abs(r3)*ao
eB3=-angle(r3)
etaB1=aB1*cos(theta-eB1)
etaB2=aB2*cos(theta-eB2)
```

```
etaB3=aB3*cos(theta-eB3)
CDL11=sqrt(ao/(max(etao-etaB1)*F1))
CDL22=sqrt(aB1/(max(etaB1-etaB2)*F2))
CDL33=sqrt(ao/(max(etao-etaB1)*F3))
CDL44=sqrt(aB1/(max(etaB1-etaB3)*F4))

C11=CDL1*Ac1/AB1*sqrt(2*g/ao)
C22=CDL2*Ac2/AB2*sqrt(2*g/aB1)
C33=CDL3*Ac3/AB1*sqrt(2*g/ao)
C44=CDL4*Ac4/AB3*sqrt(2*g/aB1)

%velocity in the inlet
uc1=sqrt(2*g/ao)*CDL1*(etao-ao*r1)
uc1max=abs(uc1)
ev1=-angle(uc1)
uc2=sqrt(2*g/aB1)*CDL2*(ao*r1-ao*r2)
uc2max=abs(uc2)
ev2=-angle(uc2)
uc3=sqrt(2*g/ao)*CDL3*(etao-ao*r1)
uc3max=abs(uc1)
ev3=-angle(uc1)
uc4=sqrt(2*g/aB1)*CDL4*(ao*r1-ao*r3)
uc4max=abs(uc4)
ev4=-angle(uc4)
%END
```

APPENDIX B
INLET HYDRAULICS RELATED DERIVATIONS

B.1 Linearization of Damping Term

The linearization of the damping term in Eq. (3.6) is done as given in Bruun (1978). The bay tide response is represented by

$$\eta_B = a_B \sin(\theta - \varepsilon_B) \tag{B.1}$$

where

$\theta = \dfrac{2\pi t}{T} = \sigma t$, dimensionless time.

a_B = one-half the tide range (i.e., amplitude) in the bay, and

ε_B = lag between high water (HW) or low water (LW) in the ocean and corresponding HW or LW in the bay. Also,

$$\eta_o = a_o \sin(\theta) \tag{B.2}$$

from the continuity equation we further have

$$A_c u = A_B \frac{d\eta_B}{dt} \tag{B.3}$$

where A_c is the area of cross-section of the inlet and A_B is the surface area of the bay.

The time of HW or LW in the bay, i.e., when $\dfrac{d\eta_B}{dt} = 0$, coincides with time of slack water, i.e., $u = 0$, so that ε_B is also the lag of slack water after HW or LW in the ocean. Thus it can be written as

$$\frac{d\eta_B}{dt}\left|\frac{d\eta_B}{dt}\right| = \sigma^2 a_B{}^2 \cos\left(\theta - \varepsilon_B\right)\left|\cos\left(\theta - \varepsilon_B\right)\right| \tag{B.4}$$

or in terms of Fourier series Eq. (B.4) can be written as

$$\frac{d\eta_B}{dt}\left|\frac{d\eta_B}{dt}\right| = \sigma^2 a_B{}^2 \sum_{n=1}^{n=\infty} \frac{8\sin\left(\frac{n\pi}{2}\right)}{n\pi\left(4-n^2\right)} \cos n\left(\theta - \varepsilon_B\right) \tag{B.5}$$

where n takes only odd integral values. For linearization purposes n=1, so that Eq. (B.5) becomes

$$\frac{d\eta_B}{dt}\left|\frac{d\eta_B}{dt}\right| = \sigma^2 a_B{}^2 \frac{8}{3\pi} \cos n\left(\theta - \varepsilon_B\right) \tag{B.6}$$

The amplitude of the tidal velocity is given by

$$u_{\max} = \frac{a_B \sigma A_B}{A_c} \tag{B.7}$$

Therefore, it can be written as

$$u|u| = \frac{8}{3\pi} u_{\max} u \tag{B.8}$$

where $u_{\max}$ is the amplitude of the u.

B.2 Shear Stress Dependence on Area

For each inlet discharge is defined as a time varying function:

$$Q_i(t) = \frac{A_{Bi}}{A_i} \frac{d\eta_B}{dt} \tag{B.9}$$

$$Q_i(t) = \pm A_i \sqrt{\frac{2gR_i}{m_i R_i + 2F_i L_i}} \sqrt{|\eta_o - \eta_{Bi}|} \tag{B.10}$$

The expression for maximum tidal velocity can be obtained by the solution of the above equations with the simplifying assumptions mentioned in Chapter 2.

$$u_{\max i} = C(K) \sin\gamma \frac{2\pi A_B a_o}{AT} \frac{K_i}{K} \tag{B.11}$$

where K is the coefficient of repletion,

$$K_i = \frac{T}{2\pi a_o}\frac{A_i}{A_B}\sqrt{\frac{2gR_i a_o}{m_i R_i + 2F_i L_i}} \tag{B.12}$$

and

$$K = \sum K_i \tag{B.13}$$

is summation is over all the inlets. The function $C(K)\sin\gamma$ is a monotonically increasing function with C=0 for K=0 and C=1 for K=∞, γ is a specific time when sea is at MSL, as defined by Kuelegan (1951)

It is seen below that the bottom shear stress, $\hat{\tau}$, varies strongly with the cross-sectional area. This can be shown with the help of approximate analytical solution carried out by Keulegan (1951). Substituting the value of u from Eq. (B.11) in Eq. (3.1), and taking $C(K)\sin\gamma$; 1 and F = 0.003:

$$\hat{\tau}\ ;\ \rho F\left[\frac{2\pi a_o A_B}{T}\right]\frac{1}{A^2} \tag{B.14}$$

It is clear from the above equation that $\hat{\tau}$ has a strong dependence on A.

B.3 General Equation for hydraulic radius.

Consider the general trapezoidal cross-section:

Area, $A = \frac{1}{2}\left(B + B_0\right)h = \frac{1}{2}Bh\left(1 + \frac{B_0}{B}\right)$

Wetted perimeter, $P = B_0 + 2\sqrt{\frac{1}{4}(B - B_0)^2 + h^2} = B\left(\frac{B_0}{B} + \sqrt{\left(1 - \frac{B_0}{B}\right)^2 + 4\left(\frac{h}{B}\right)^2}\right)$

Hydraulic radius, $R = \frac{A}{P} = \dfrac{\frac{1}{2}h\left(1 + \frac{B_0}{B}\right)}{\frac{B_0}{B} + \sqrt{\left(1 - \frac{B_0}{B}\right)^2 + 4\left(\frac{h}{B}\right)^2}}$

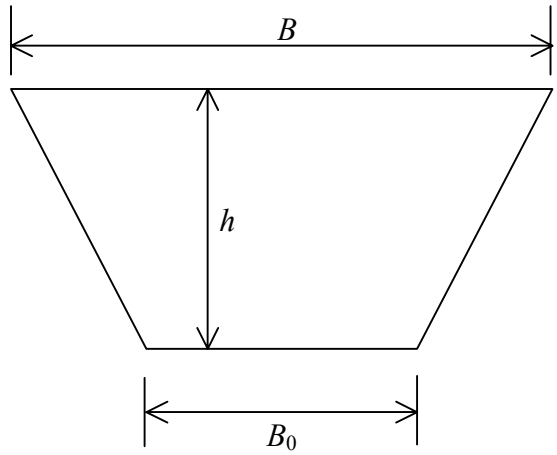

Figure B.1 Trapezoidal Cross-section

Now consider two cases: 1) Rectangular cross-section, i.e., $B_0 = B$, and 2) Triangular cross-section, i.e., $B_0 = 0$.

B.3.1 Rectangular

$B=B_0$, Therefore hydraulic radius for a rectangle is

$$R = \frac{A}{P} = \frac{h}{1+2\left(\frac{h}{B}\right)}$$

B.3.2 Triangular

For triangular section, $B_0=0$

$$R = \frac{A}{P} = \frac{\frac{1}{2}h}{\sqrt{1+4\left(\frac{h}{B}\right)^2}}$$

B.4 Hydraulic Radius for Triangular Cross-Section

For a triangular cross-section the hydraulic radius is related as a square root of the area, as shown below:

Figure B.2 is a triangular cross-section where β is the angle with the horizontal on both the sides:

Area $A = \frac{1}{2} h 2h \tan\beta$

Wetted perimeter $P = \frac{2h}{\cos\beta}$

Hydraulic radius $R = \frac{A}{P} = \frac{1}{\sqrt{2\sin\beta\cos\beta}}\sqrt{A} = a\sqrt{A}$ (B.15)

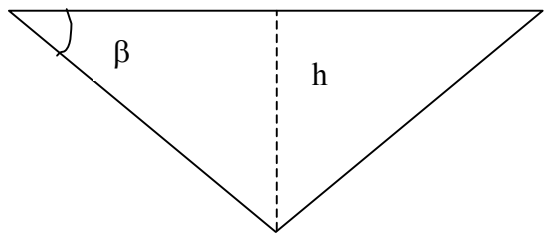

Figure B.2 Triangular cross-section.

APPENDIX C
CALCULATION OF BAY TIDE AND LINEAR DISCHARGE COEFFICIENTS

This appendix contains sample calculations of input data in Table 5.4 for the Matlab Program –2 (Appendix A) in Chapter 5. Estimation of bay tide amplitude (a_{B1}, a_{B2}, a_{B3}), input for Table 5.4 was made by taking the weighted-averages of the NOS tide amplitudes at reported stations in the bay. Let us take the case of St. Andrew Bay (Table C.1). This bay has three stations where tide is reported. The weighting factor for the range at a given station was estimated by selecting the approximate area of influence of tide (range) surrounding that station. Given the tidal period of 12.42 h, the phase difference between Gulf and the bay could be converted in to degree or radians.

Table C.1 Weighted-average bay tide ranges and phase differences

St. Andrew Bay					
Station	Weighting factor	Sept. tide range (m)	Weighted-average (m)	Phase difference (h)	Weighted-average (h)
Channel Entrance	0.48	0.197	0.0945	0.0017	0.008
Panama City	0.37	0.203	0.0751	1.0000	0.370
Parker	0.15	0.236	0.0354	2.0000	0.300
Total			0.2050		0.678 h=19.65^{o}
East Bay					
Laird Bayou	0.40	0.236	0.0940	2.0000	0.800
Parker	0.40	0.236	0.0940	2.0000	0.800
Panama city	0.20	0.203	0.0406	1.0000	0.200
			0.2300		1.8 h=52.17^{o}
West Bay					
West Bay Creek	0.50	0.236	0.118	3.0000	1.5 hrs
Lynn Haven	0.50	0.236	0.118	2.0000	1.0 hrs
			0.236		2.5 h=72.46^{o}

The Gulf tide range had to be estimated, as there was no open coast tidal station near to the study site. The procedure was as follows:

1 The tidal range at the gauge installed by UF in September 2001 in the bay was R = 0.18m.

2 The kinetic head in the channel was calculated by using the peak velocity value, 0.63 m/s:

$$h_k = \frac{u^2}{2g} = \frac{(0.63)^2}{2*9.81} = 0.02 \text{ m.}$$

3 Thus the Gulf tide range was obtained as $R_o = R + h_k = 0.02 + 0.18$ m.

So the amplitude correction factor $\frac{R_o}{R} = \frac{0.20}{0.18} = 1.11$

4 The distance between the open coast (Gulf-ward tips of the entrance jetties) and the UF gauge was X = 673 m and the depth of the deepest channel (thalweg) between the two locations h =12 m.

5 Therefore the time difference between calculated ocean tide and the bay is calculated as $\frac{X}{\sqrt{gh}} = \frac{673}{\sqrt{9.81*12}} = 62.03\,\text{s} = 1.03\,\text{min}$

The maximum driving heads, $(\eta_o - \eta_{B1})_{max}$, $(\eta_{B1} - \eta_{B2})_{max}$ $(\eta_{B1} - \eta_{B3})_{max}$ are calculated as suggested by O'Brien and Clark (1973).

1 The driving head between ocean and bay 1 $(\eta_o - \eta_{B1})_{max}$, at any time t during the tidal cycle is

$$\eta_o - \eta_{B1} = a_o \cos\sigma t - a_{B1}\cos(\sigma t - \varepsilon_{B1}) \tag{C.1}$$

slack water occurs at $\sigma t = \varepsilon_{B1}$

Maximum head occurs at $\sigma t = \varepsilon_{B1} + \frac{\pi}{2}$

$$\therefore (\eta_o - \eta_{B1})_{\max} = a_o \sin\varepsilon_{B1} \tag{C.2}$$

2 The driving head between bay1 and bay 2 $(\eta_{B1} - \eta_{B2})_{max}$, at any time t during the tidal cycle is

$$\eta_{B1} - \eta_{B2} = a_{B1}\cos(\sigma t - \varepsilon_{B1}) - a_{B2}\cos(\sigma t - \varepsilon_{B2}) \tag{C.3}$$

slack water occurs at $\sigma t = \varepsilon_{B2} - \varepsilon_{B1}$

Maximum head occurs at $\sigma t = \frac{\pi}{2} + \varepsilon_{B2} - \varepsilon_{B1}$

$$\therefore \left(\eta_{B1} - \eta_{B2}\right)_{\max} = a_{B1}\cos\left(\frac{\pi}{2} + \varepsilon_{B2} - \varepsilon_{B1} - \varepsilon_{B1}\right) - a_{B2}\cos\left(\frac{\pi}{2} + \varepsilon_{B2} - \varepsilon_{B1} - \varepsilon_{B2}\right) \quad \text{(C.4)}$$

$$\therefore \left(\eta_{B1} - \eta_{B2}\right)_{\max} = -a_{B1}\sin\left(\varepsilon_{B2} - 2\varepsilon_{B1}\right) - a_{B2}\sin\left(\varepsilon_{B1}\right) \quad \text{(C.5)}$$

For maximum head difference we have to take absolute value of the head difference. Examples of the use of the above equations are shown in Figures C.1 and C.2. Figure C.1 gives the ocean and bay 1 tide head difference, while Figure C.2 gives the head difference between bay 1 and bay 2. Table C.2 provides the values used to calculate the linear discharge coefficients given by Eqs (2.28), (2.29) and (2.50).

Table C.2 Calculation of $(\eta_o - \eta_{B1})_{max}$, $(\eta_{B1} - \eta_{B2})_{max}$ $(\eta_{B1} - \eta_{B3})_{max}$

Sept. 2001 tide	Ampl (m)	Phase diff. with Gulf (deg)	Tide functions	Max. tide difference (m)
Ocean	0.1090[a]	00.00	$\eta_o = 0.109\cos(\theta)$	-
Bay 1	0.1025	19.65	$\eta_{B1} = 0.1025\cos(\theta + 19.65^0)$	$\left(\eta_o - \eta_{B1}\right)_{\max} = 0.0366$
Bay 2	0.1150	52.17	$\eta_{B2} = 0.115\cos(\theta + 52.17^0)$	$\left(\eta_o - \eta_{B1}\right)_{\max} = 0.0601$
Bay 3	0.1180	72.46	$\eta_{B3} = 0.118\cos(\theta + 72.46^0)$	$\left(\eta_o - \eta_{B1}\right)_{\max} = 0.0989$

[a] Amplitude correction factor of 1.11 applied.

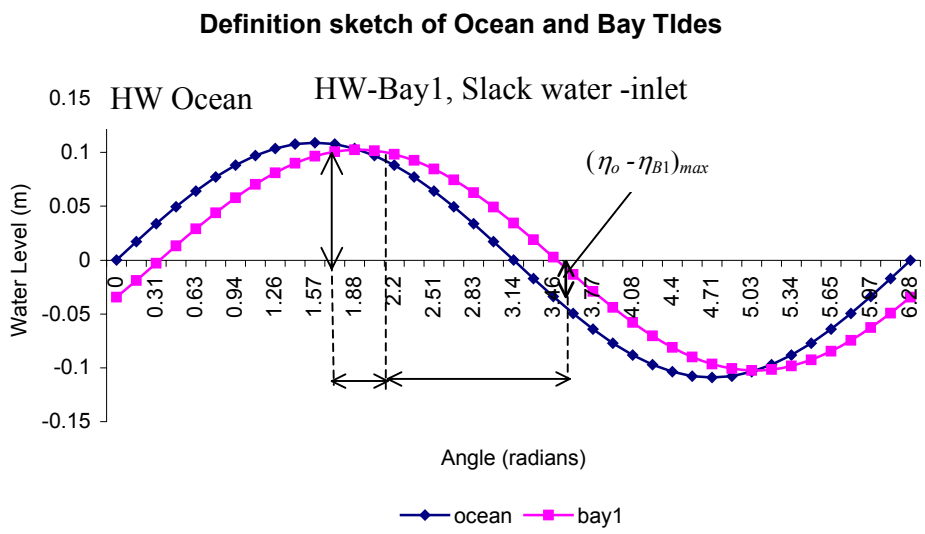

Figure C.1 Head difference between ocean (Gulf) and bay 1.

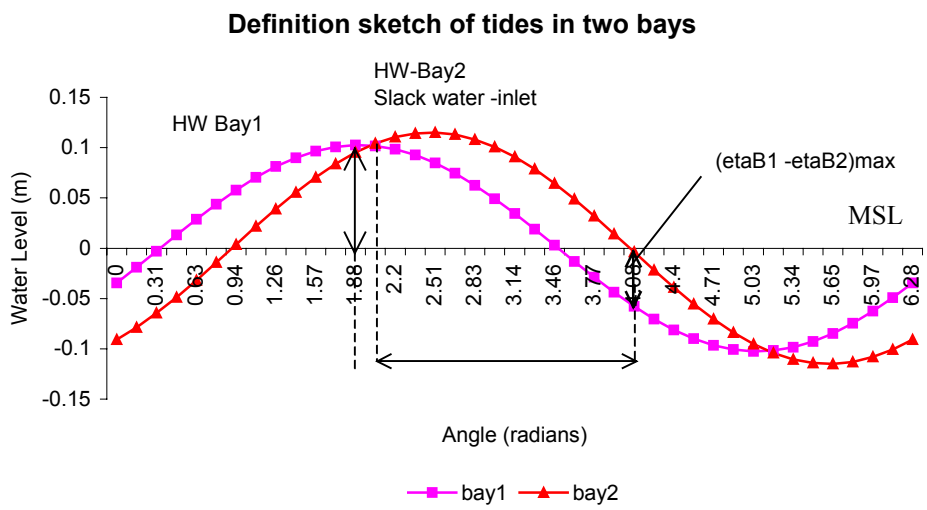

Figure C.2 Head difference between bay1 and bay 2.

APPENDIX D
CALCULATIONS FOR STABILITY ANALYSIS

D.1 Introduction

van de Kreeke's (1990) linearized lumped model is used for development of the equilibrium flow curves for the two inlets, namely St. Andrew Entrance and East Pass. This appendix includes the calculation of some of the input parameters listed in Table 5.6

D.2 Calculations

D.2.1 Equilibrium velocity

The equilibrium velocity is calculated using Eq. (D.1), which is same as Eq. (3.12). The equilibrium shear stress, $\hat{\tau}_{eq}$, is taken from Mehta and Christensen (1983).

$$u_{eqi} = \sqrt{\frac{\tau_{eqi}}{8/3\pi\rho F_i}} \tag{D.1}$$

Table D.1 Calculation of equilibrium velocity

Friction Coefficient, F=f/8	Range of $\hat{\tau}_{eq}$ (Pa)	ρ, Density (kg/m^3)	Range of u_{eq} (m/s)
0.003	0.48-0.72	1024	0.43-0.52
0.004	0.48-0.72	1024	0.37-0.45

D.2.2 Constant for Triangular schematization.

The constant a_i [Appendix B, Eq (B.15)] is calculated for St. Andrew Bay Entrance and East Pass.

Table D.2 Calculation of a_i

Inlet	Cross-sectional Area (m^2)	Hydraulic Radius, R (m)	$a_i = \frac{R_i}{\sqrt{A_i}}$
St. Andrew Bay Entrance	5,250	10	0.138
East Pass	255	3	0.187

D.3 Relationship between Flow Curves and Stability of Two Inlets

In general, equilibrium areas of the two inlets are defined by the sets of the areas where the two inlet equilibrium flow curves intersect. The hatched rectangle (common equilibrium zone) is formed by the intersection of two equilibrium intervals. Each interval is defined from the first equilibrium area to ∞. Consider the following two cases:

1 For both inlets to be in equilibrium, it is necessary that the enhanced parts of both the curves intersect. The hatched portion is the common equilibrium region where both the inlets are stable. Suppose after a storm, point **a** (Figure. D.1) marked by a square (in hatched region) represent the areas of the two inlets. If we follow the arrows, which show how the areas of the inlets try to adjust after the storm, it is clear that both the areas lie in the enhanced parts, so both the inlets will be stable.

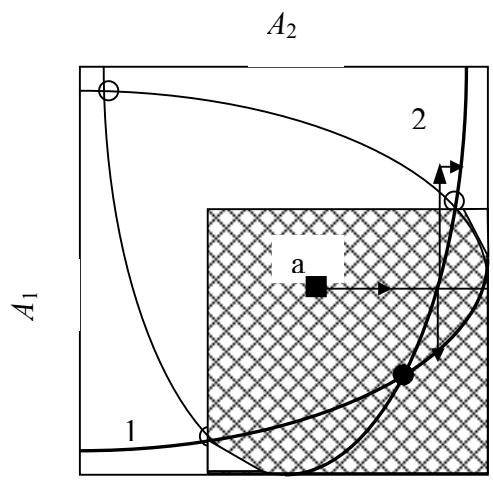

Figure D.1 General configuration of equilibrium flow curve.

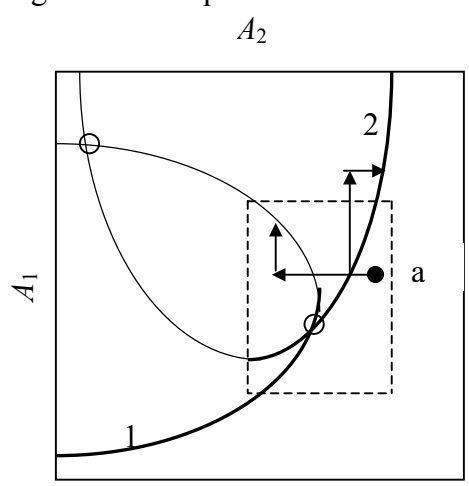

Figure D.2 General configuration of equilibrium flow curve.

2 In this set of equilibrium flow curves, although the enhanced parts of the equilibrium curves intersect, the inlets need not necessarily come back to the equilibrium region. Let's draw a rectangle around the intersection of enhanced part of the equilibrium flow curve. Let us take a point **a** (Figure. D.2), which represents the areas of the inlets just after a storm event. In this case following the arrows, it is clear that Inlet 2 will reach stable equilibrium but Inlet 1 will not. So this set of equilibrium flow curves does not always represent a stable equilibrium. Similarly we can argue with the other Figures (Figure 3.5 (c) and Figure 3.5 (d) in Chapter 3)

D.4 Matlab Programs

For solving the linearized model for stability, two Matlab programs were developed, Program –1 for solving the inlets with rectangular cross-section and Program –2 for triangular cross-section.

D.4.1 Program-1

```
%UNIVERSITY OF FLORIDA
%DEPARTMENT OF CIVIL AND COASTAL ENGINEERING
%INLET STABILITY CALCULATION ASSUMING THE CROSS-SECTION TO BE RECTANGULAR


clear all
Ab=90*10^6;%Bay surface area, St. Andrew
eta_o=0.26;%Ocean Tide amplitude
ueq1=0.40;%Equilibriuim velocity in Inlet 1 , as calculated in Appendix D.
ueq2=0.45;%Equilibriuim velocity in Inlet 2 , as calculated in Appendix D.
T=18;%Tidal Period
sigma=(2*pi)/(T*3600);
g=9.81;%acceleration due to gravity

% Inlet -1
W1=525;% Width of the Inlet-1
L1=1340;% Length of the Inlet-1
F1=4*10^(-3);%Friction coefficient
%a1=0.044;

% Inlet-2
B=[];
W2=300; %Width of Inlet-2
L2=2000;%Length of the Inlet-2
F2=0.004;%Friction Coefficient of Inlet-2
%a2=0.197;
```

```
A=[];
P1=Ab*sigma*(eta_o)^2;
P2=(2*8*(F1*L1*W1*(ueq1^3)+F2*L2*W2*(ueq2^3)))/(3*pi*g);
if P1>P2
   sprintf('the solution to the inlet system is possible')
else

   sprintf('the solution to the inlet system is not possible')
end


a=(F1*L1*W1*(ueq1^3)+F2*L2*W2*(ueq2^3))^2;
b=-(Ab*sigma*(eta_o))^2;
c=((Ab*sigma*8)/(3*pi*g))^2;
p=[a b c ];
roots(p)
A1eq=sqrt(((F1*L1*W1*(ueq1^2))^2)*roots(p))
A2eq=sqrt(((F2*L2*W2*(ueq2^2))^2)*roots(p))

%B1=(A1.^-1).*2*F1*L1*W1;
newm1=[];

%Solve for inlet 1
for i=1:80
   A2=i*100;
   % for equilibirium case B1*ueq1^2=B2*ueq2^2
a1=ueq1^2;
b1=2*A2*ueq1*ueq2;
c1=(ueq1^2)*(A2^2)-(Ab*sigma*eta_o)^2;
d1=0;
e1=((8*Ab*sigma*F1*L1*W1*ueq1^2)/(3*pi*g))^2;

p1=[a1 b1 c1 d1 e1];
Af(1:4)=roots(p1);
B=[A2 A2 A2 A2;Af(1:4)];
newa=B(3:6);
newm=reshape(newa,2,2);
newm1=cat(2,newm,newm1);
fid = fopen('r1.txt','w');
fprintf(fid,'%6.2f  %12.8f\n',newm1);
fclose(fid);
end
newm12=[]
%Solve for inlet 2
for i=1:80
   A1=i*100;
```

```
  % for equilibirium case B1*ueq1^2=B2*ueq2^2
a2=ueq2^2;
b2=2*A1*ueq1*ueq2;
c2=(ueq2^2)*A1^2-(Ab*sigma*eta_o)^2;
d2=0;
e2=((8*Ab*sigma*F2*L2*W2*ueq2^2)/(3*pi*g))^2;

p2=[a2 b2 c2 d2 e2];
As(1:4)=roots(p2);
B2=[A1 A1 A1 A1;As(1:4)];
newa2=B2(3:6);
newm2=reshape(newa2,2,2);
newm12=cat(2,newm2,newm12);
fid = fopen('r2.txt','w');
fprintf(fid,'%6.2f  %12.8f\n',newm12);
fclose(fid);
end

%Line
A2L=0:100:2000;
A1L=(F1*L1*W1*A2L)./(F2*L2*W2);

eq1=[A2L;A1L]
fid = fopen('r3.txt','w');
fprintf(fid,'%6.2f  %12.8f\n',eq1);
fclose(fid);
%End
```

D.4.2 Program-2

```
%UNIVERSITY OF FLORIDA
%DEPARTMENT OF CIVIL AND COASTAL ENGINEERING
%INLET STABILITY CALCULATION ASSUMING THE CROSS-SECTION TO BE
TRIANGULAR

clear all

%Input Parameters

Ab=90*10^6;%Bay surface area, St. Andrew
eta_o=0.26;%Ocean Tide amplitude
ueq1=0.4;%Equilibriuim velocity in Inlet 1 , as calculated in Appendix D.
ueq2=0.45;%Equilibriuim velocity in Inlet 2 , as calculated in Appendix D
T=18;%Tidal Period
sigma=2*pi/(T*3600);
g=9.81;%acceleration due to gravity
```

```
%Inlet 1
L1=1340;%Length of Inlet
R1=10;% Hydraulic Radius
F1=4*10^-5%k+(f*L1)/(4*R1);%friction factor F includes ken kex fL/4R
alpha1=0.138;%factor for triangular cross-section calculated as alpha=R/sqrt(Area)
B=[];

%Inlet 2
L2=2000;%Length of Inlet
R2=3;% Hydraulic Radius
F2=0.004;%friction factor F includes ken kex fL/4R
alpha2=0.187;%factor for triangular cross-section calculated as alpha=R/sqrt(Area)
A=[];

%calculations

P1=Ab*sigma*(eta_o)^3;
P2=((3*sqrt(3))/2)*((8/(3*pi))^2)*(((F1*L1*(ueq1^5))/(alpha1*g))^2+((F2*L2*(ueq2^5)
)/(alpha2*g))^2);
if P1>P2
  sprintf('the solution to the inlet system is possible')
else

  sprintf('the solution to the inlet system is not possible')
end

%Solve for the 2 roots , its a third degree polynomial so lets define the coefficients

a=(ueq1*(((F1*L1*alpha1)/(F1*L1*alpha1))^2)+ueq2*(((F2*L2*alpha1)/(F1*L1*alpha2
))^2))^2;
b=0;
c=-(Ab*sigma*eta_o)^2;
d=((8/(3*pi))*(Ab*sigma)*((F1*L1)/(alpha1*g))*(ueq1^2))^2;
p=[a b c d];
roots(p)
A(1:3)=roots(p);
A1=A(2:3);
% for equilibirium case B1*ueq1^2=B2*ueq2^2

A2=((((alpha1*F2*L2)/(alpha2*F1*L1))*((ueq2/ueq1)^2))^2)*A1;

%B1=(A1.^-1).*2*F1*L1*W1;
newm1=[];

%Equilibrium curve for Inlet 1
for i=1:100
```

```
   A2=i*100;
a1=ueq1^2;
b1=2*A2*ueq1*ueq2;
c1=(ueq1^2)*(A2^2)-(Ab*sigma*eta_o)^2;
d1=((8*Ab*sigma*F1*L1*ueq1^2)/(alpha1*3*pi*g))^2;

p1=[a1 b1 c1 d1];
roots(p1);
Af(1:3)=roots(p1);
B=[A2 A2 A2;Af(1:3)];
newa=B(3:6);
newm=reshape(newa,2,2);
newm1=cat(2,newm,newm1);
fid = fopen('t1.txt','w');
fprintf(fid,'%6.2f  %12.8f\n',newm1);
fclose(fid);
end

newm12=[];
%Equilibrium curve for Inlet 2
for i=1:100
   A1=i*100;
a2=ueq2^2;
b2=2*A1*ueq1*ueq2;
c2=(ueq2^2)*(A1^2)-(Ab*sigma*eta_o)^2;
d2=((8*Ab*sigma*F2*L2*ueq2^2)/(alpha2*3*pi*g))^2;
p2=[a2 b2 c2 d2];
roots(p2);
As(1:3)=roots(p2);
B=[A1 A1 A1;As(1:3)];
newa2=B(3:6);
newm2=reshape(newa2,2,2);
newm12=cat(2,newm2,newm12);
fid = fopen('t2.txt','w');
fprintf(fid,'%6.2f  %12.8f\n',newm12);
fclose(fid);
end
%Line
A2L=0:100:7000;
A1L=((F1*L1*alpha2*(A2L.^0.5))./(F2*L2*alpha1)).^2;
eq1=[A2L;A1L]
fid = fopen('t3.txt','w');
fprintf(fid,'%6.2f  %12.8f\n',eq1);
fclose(fid);
    %end.
```

LIST OF REFERENCES

Aubrey, D. G., and Weishar, L. (eds), 1988. *Hydrodynamics and Sediment Dynamics of Tidal Inlets*. Lecture Notes on Coastal and Estuarine Studies Vol. 29, Springer-Verlag, New York.

Becker, M. L., and Ross, M. A., 2001. Interaction of tidal inlets in a multi-inlet bay system: A case study along the central Gulf Coast of Florida. *Journal of Coastal Research*, 17(4), pp. 836-849

Brunn, P., 1978. *Stability of Tidal Inlets*. Elsevier, Amsterdam.

Dean, R. G., 1983. Hydraulics of inlets, *Report UFL/COEL-83/004*, Coastal and Oceanographic Engineering Department, University of Florida, Gainesville.

Escoffier, F. F., 1940. The stability of tidal inlets. *Shore and Beach*, 8(4), 114-115.

Escoffier, F. F., and Walton, T. L., 1979. Inlet stability solutions for tributary inflow. *Journal of the Waterways, Port, Coastal and Oceanographic Division, ASCE,* 105(4), 341-355.

Jain, M., and Mehta, A. J., 2001. Hydrographic measurements at St. Andrews Bay Entrance, Bay County, Florida. *Report UFL-COEL-2001/014*, Coastal and Oceanographic Engineering Program, Department of Civil and Coastal Engineering, University of Florida, Gainesville.

Jain, M., and Mehta, A. J., 2002. Hydrographic measurements at St. Andrews Bay Entrance and East Pass, Bay County, Florida, Part II. *Report UFL-COEL-2002/010*, Coastal and Oceanographic Engineering Program, Department of Civil and Coastal Engineering, University of Florida, Gainesville.

Jain, M., Paramygin, V. A., and Mehta, A. J., 2002. Hydrographic measurements at St. Andrews Bay Entrance and East Pass, Bay County, Florida, Part I. *Report UFL/COEL-2002/001*, Coastal and Oceanographic Engineering Program, Department of Civil and Coastal Engineering, University of Florida, Gainesville.

Jarrett, J. T., 1976 Prism-inlet area relationships. *G.I.T.I Report No. 3*, U.S. Army Engineering Coastal Engineering Research Center, Ft. Belvoir, VA.

Keulegan, G. H., 1951, Third Progress Report on Tidal flow in entrances. Water Level fluctuations of basins in communication with seas. *Report No. 1146, National Bureau of Standards, U. S Department of Commerce,* Washington, D. C. pp 32.

Keulegan, G. H., 1967, Tidal flows in entrances: Water level fluctuations of basins in communication with the seas. *Committee on Tidal Hydraulics Technical Bulletin No. 14*, U.S. Army Engineer Waterways Experiment Station, Vicksburg, MS.

Mehta, A. J., 1975. A long term stability criterion for inlets on sandy coasts. *Report UFL/COEL-1975/0018*, Coastal and Oceanographic Engineering Laboratory, University of Florida, Gainesville.

Mehta, A. J. and Christensen, B. A., 1983, Initiation of sand transport over coarse beds in tidal entrances. *Coastal Engineering*, 7, 61-75.

O'Brien, M. P., 1931. Estuary tidal prisms related to entrance area, *Civil Engineering*, 1(8), 738-739.

O'Brien, M. P., 1969. Equilibrium flow areas of inlets on sandy coasts. *Journal of Waterways and Harbors Division, ASCE*, 95(1), 43-52.

O'Brien, M. P. and Clark, R. P., 1973. Hydraulic constants of tidal entrances I: Data from NOS Tide Tables, Current Tables and navigational charts. *Technical Report No. 21*, Coastal and Oceanographic Engineering Laboratory, University of Florida, Gainesville.

O'Brien, M. P. and Dean, R. G., 1972. Hydraulic and sedimentary stability of coastal inlets. *Proceedings of the 13th International Conference on Coastal Engineering*, *ASCE*, Vol. 2, New York, 761-780.

van de Kreeke, J., 1967. Water level fluctuations and flow in tidal inlets. *Journal of Waterways and Harbors Division*, *ASCE,* 93(4), 97-106.

van de Kreeke, J., 1985. Stability of tidal inlets - Pass Cavallo, Texas. *Estuarine, Coastal and Shelf Science,* 21, 33-43.

van de Kreeke, J., 1988. Hydrodynamics of tidal inlets. In: *Hydrodynamics and Sediment Dynamics of Tidal Inlets*, Aubrey, D.G. and Weishar, L., eds, Springer-Verlag, New York, 1-23.

van de Kreeke, J., 1990. Can multiple tidal inlets be stable? *Estuarine, Coastal and Shelf Science,* 30, pp 261-273.

BIOGRAPHICAL SKETCH

Mamta Jain was born in 1976, as the only daughter of Kanta and Mohan Jain, in Kathmandu, Nepal. She did her bachelor's in civil engineering from Delhi College of Engineering in 1998. After that she worked for three years as Ocean Engineer in the oil sector consultancy, Engineers India Ltd. Her main area of specialization is design of oil terminals. The craving for more knowledge made her take a break from the job and she applied to graduate school. In fall 2001 she was admitted to the Graduate School of the University of Florida. She married Parag Singal in December 2001, who encouraged and supported her to continue her academic work in the Coastal and Oceanographic Engineering Program of the Department of Civil and Coastal Engineering.